Development of PTSD-like behavior in adult mice after observing an acute traumatic event

Ray X. Lee,[1,2]* Greg J. Stephens,[2,3] Bernd Kuhn[1]

Affiliations:

[1] Optical Neuroimaging Unit, Okinawa Institute of Science and Technology (OIST) Graduate University, Okinawa, Japan.

[2] Biological Physics Theory Unit, OIST Graduate University, Okinawa, Japan.

[3] Department of Physics and Astronomy, Vrije Universiteit Amsterdam, Amsterdam, The Netherlands.

* Correspondence to: rayxin.lee@oist.jp

Abstract: For post-traumatic stress disorder (PTSD) in humans, it remains a major conceptual challenge how stress reactions emerge after a protracted symptom-free period. Here, we study the behavioral development in mice isolated after observing a traumatic event inflicted upon their pair-housed partners. Fine-scale behavioral analysis showed that anxiety-related reactions gradually increased more in traumatized mice during isolation than in mice isolated without traumatic experience. These increases in anxiety-related reactions were independent of fear memory. Interestingly, instead of social avoidance from anxiety, traumatized mice showed long-term reduction of social interest to strangers. These behaviors were not observed if the traumatic event happened to a stranger mouse. Additionally, traumatized mice showed rebound responses to their partners after 4 weeks of separation. This suggests that affectional bonding as the single common factor underlies the otherwise independent development of PTSD-like behaviors in this paradigm. This conclusion is also supported by the strengthening of an anterior cingulate cortex (ACC)-centered network revealed by diffusion tensor imaging.

Introduction

Post-traumatic stress disorder (PTSD) is one of the most prevalent mental health disorders [1,2]. Although the mechanisms underlying PTSD are not well understood [3], a core belief shared across various hypotheses is to view PTSD as an association between trauma-induced states such as fear memory, increased anxiety, and social withdrawal [4–8]. In this collective model (Figure 1A), behaviors slowly change and influence each other during the stress incubation period until a new, abnormal equilibrium is reached. This new equilibrium is described by PTSD.

To identify the basic psychopathological mechanisms during stress incubation, it is beneficial to use an experimental assay with purely psychosocial manipulations on controlled subjective experiences and a homogeneous genetic background. Laboratory rodents proved to be a reliable model system for such a purpose. Behavioral studies revealed that laboratory rodents engage in advanced social behaviors and show similar psychological states as humans [9–12]. Specifically, laboratory rodents have been used to study stress behavior and the pharmacology of stress [13–16]. Also, a delay period before showing substantial stress reactions was reported in the context of rodent models simulating human PTSD [17–21]. Stress reactions have been studied with a wide variety of aversive stimuli, ranging from acute physical stress [22,23] to a prolonged period of repeated social defeat through witnessing [19,24]. A time-dependent amplification of fear expression [25] has been proposed to explain generalized avoidance, including associative fear conditioning or non-associative fear sensitization, through stress incubation in rodents [18]. The variability of emergent phenotype following trauma was proposed to be an interaction of incubated stress and fear conditioning [21].

Here, we combined behavioral scenarios, analytic methods, and psychological hypotheses to study the development of stress incubation by psychobehavioral experiments in mice. Additionally, we analyzed morphological changes of the brain due to stress incubation by diffusion tensor imaging (DTI). We propose that a single factor, affectional bonding, plays

50 a dominant role during the stress incubation period towards the development to PTSD-like
51 behavior. In this unitary model (Figure 1B), a single common factor underlies the otherwise
52 diverse and independent development of post-traumatic behaviors in mice.

53

54 **Results**

55 ***Emergence of long-term effects after trauma induction***

56 To identify post-traumatic behavioral development with minimal physical impact and
57 peri-traumatic contribution, we developed the following assay of an acute witnessing trauma
58 (Figure 2A): Partnership between the male focal mouse and its male partner was established
59 by housing them together for 3 weeks (Day-21–Day0). During this pair-housing, the mice slept
60 together in a single nest which they built, and no aggressive interaction was observed. On
61 Day0 (trauma induction), the focal mouse observed its partner being attacked by 5 different
62 aggressor mice in succession (aggressive encounters) and stayed together with the attacked
63 partner between each aggressive encounter (stress infiltration and resting). Importantly, the
64 focal mouse only experienced the traumatic event by witnessing the attacks and by social
65 communication, but not through any direct physical threat, such as attack bites and pursuits
66 from either the aggressors or its partner. After the last aggressive encounter, the focal mouse
67 (Partner-observing mouse) was socially isolated for 4 weeks (Day0–Day28). Behavior was
68 tested on Days -7, 1, 7, and 28.

69 To differentiate behavioral consequences from the trauma induction and the effects of
70 isolation, adaptation to the tests, and aging, a control group of mice were isolated from their
71 partners on Day0 without trauma induction (No-scenario-isolated mice; Figure 2B). We found
72 that Partner-observing mice (n = 47) built nests with significantly higher walls than those
73 constructed by No-scenario-isolated mice (n = 47) after isolation (Figure 2C). Partner-
74 observing mice also increased their body masses in the late phase of the study (Figure 2D).

Both observations indicate a long-term effect of the trauma. These differences could be alternatively explained, e.g. having better emotional stability and therefore nicer nests and better appetites *v.s.* manifesting protective responses of anxiety by hiding behind higher nest walls and engaging in anxiety-induced binge eating [26,27]. However, the corticosterone concentrations in blood plasma [28] confirms increased stress in the Partner-observing mice: Compared with No-scenario-isolated mice, Partner-observing mice showed higher baseline plasma corticosterone level after trauma, which reached statistical significance on Day28 (Figure 2E). To confirm the stress reactions suggested by the baseline plasma corticosterone level, in this experiment, we also isolated the attacked mice and collected their blood samples after trauma (Attacked mice; n=5, note that 2 out of 5 mice died on Days 4 and 5, supposedly due to a serious depression-like anorexia as no obvious physical trauma occurred; interestingly, such losses were not observed in attacked mice which were subsequently group-housed). The tendency of higher baseline plasma corticosterone level was also observed in Attacked mice which had a more obvious baseline corticosterone increment during the early phase (Figure 2E), supporting the interpretation that the observed behavioral differences are behavioral phenotypes of stress.

To investigate morphological changes in the brain, we used DTI of brains collected on Day28 to analyze brain-wide microstructural differences (Figure 3; Supplemental Figures 1 to 4): Instead of a structural change in the hypothalamus [29], significant differences mainly occurred in both neocortex and hippocampus. For Partner-observing mice, compared with No-scenario-isolated mice, their DTI-based fractional anisotropy (FA; Figure 3A) was lower in anterior cerebral cortical areas including the primary somatosensory cortex, anterior cingulate cortex, and orbital cortex, but higher in posterior cerebral cortical areas including the retrosplenial cortex and the primary visual cortex. It was also higher in the hippocampus. Different measures of DTI-based water diffusivities [mean diffusivity (MD), axial diffusivity (AD), and radial diffusivity (RD); Figure 3, B to D] were generally higher in the cerebral cortex

101 and hippocampus of Partner-observing mice than in No-scenario-isolated ones. Interestingly,
102 we observed an obvious asymmetry of the brain areas: Gray matters including the cerebral
103 cortex and hippocampus showed differences in the right brain hemisphere, while white matters
104 including the corpus callosum, anterior commissure, and cingulum bundle showed differences
105 in the left brain hemisphere. The asymmetry of diffusivity between the right and left brain
106 hemispheres were significantly enhanced in the amygdala (the right more than the left) and
107 areas of the lateral cerebral cortical subnetwork including dorsolateral orbital cortex and insular
108 cortex (the left more than the right) for Partner-observing mice. These observations support
109 the idea that the emergence of long-term impacts after trauma induction arise from a higher-
110 order process of cognition and emotion.

111 ***Evidence of stress development revealed by fine-scale behavioral analysis***

112 To measure emotionality of Partner-observing mice in different phases after trauma, we
113 investigated the spontaneous behaviors of Partner-observing mice by using standard behavioral
114 testing setups. Although the generally believed validity to identify rodent emotionality in
115 standard behavioral tests has been criticized [30], spontaneous behavior in a steady environment
116 is arguably a representation of internal states such as emotion [31].

117 Here, we focus on anxiety-like reactions in mice. In humans, anxious behaviors are
118 shown when facing unexpected events or uncertain situations [32]. Behavioral tests for rodent
119 anxiety-like reactions were therefore designed to evaluate their stress reaction against their
120 willingness to explore (e.g. light-dark box and elevated plus-maze) or their activity under
121 conditions with a gradient of uncertainty (e.g. open field). We first examined spontaneous
122 behaviors in the light-dark box test (Figure 4A; n = 8 mice for each group), where the stressor
123 was a natural aversion to brightly lit areas [33]. Surprisingly, while the time spent in the light
124 area did not differ significantly between No-scenario-isolated and Partner-observing mice on
125 Day1, Partner-observing mice spent more time in the light area than No-scenario-isolated mice
126 on Days 7 and 28 (Figure 4A, left panels).

127 This result raised the following questions: (i) Did this behavioral difference start to
128 develop immediately after the traumatic event or only after a delay? (ii) What comparative
129 emotionality does this behavioral difference indicate?

130 To answer the first question (i), we examined the positions of the mice in the light-dark
131 box on a fine-scale. Emotion dynamically maps internal states and external stimuli onto a set
132 of corresponding behaviors [34], which should be reflected in the probability distribution of
133 different parameters shown during these behaviors. Based on spatial symmetry, we analyzed
134 T(x), the cumulative probability distribution of time that the mouse spent at positions along the
135 axis of the light-dark box (Figure 4A, top-right scheme and the equation, and middle panels for
136 the results). We calculated significance levels [presented as -log of p-values, -log(p)] of T(x)
137 between Partner-observing and No-scenario-isolated populations by computing position-
138 dependent population means and applying a two-tailed, two-sample Student's t-test (Figure 4A,
139 bottom-middle panels). Already on Day1, Partner-observing mice showed differences in their
140 spatial distribution, as they spent less time than No-scenario-isolated mice at the far end of the
141 dark area. This tendency increased with time: On Day 7, Partner-observing mice spent more
142 time in the light area close to the door compared to No-scenario-isolated, and then on Day 28
143 additionally on the far side of the light area. Collapsed -log(p) distributions reveal the overall
144 gradual increase in spatial preference differences (Figure 4A, right panel). Additionally,
145 Partner-observing mice maintained a higher locomotor speed compared to the gradually
146 decreasing speed of No-scenario-isolated mice (Figure 4B) and showed more transfers between
147 the boxes and shorter latencies until their first transfers from Day 1 (Figure 4C). These results
148 indicate an onset and gradual increase of behavioral differences immediately following the
149 trauma.

150 Regarding the second question (ii), these differences may reflect the hypo-sensitivity
151 to sensory harm and hyper-activity, such as the characteristic of somatic anxiety observed in
152 PTSD patients [35–37]; however, they may also simply indicate that Partner-observing mice

153 became braver and more excited. Reactions of cognitive anxiety are expected to be opposite
154 of those shown in somatic anxiety [35]. To determine whether the differences could be attributed
155 to chronic anxiety, we examined their behaviors in the elevated plus-maze test (Figure 5A; n =
156 8 mice for each group). In this test, stressors included fear of falling and exposure. After first
157 exposure on Day-7 and separation, mice spent only a fraction of the time in the open arms of
158 the maze, but with no significant difference between No-scenario-isolated and Partner-
159 observing mice (Figure 5A, left panels). However, Partner-observing mice spent increasingly
160 more time in the far end of the closed arms (Figure 5A, middle panels) and moved more slowly
161 in the elevated plus-maze after trauma induction (Figure 5B) with longer periods of freezing
162 and fewer entries to the central platform from the closed arms (Figure 5C).

163 Together, this indicates a higher anxiety level and supports the hypothesis that
164 behavioral differences are the result of chronic anxiety. Gradually increasing differences
165 between No-scenario-isolated and Partner-observing mice (Figure 5, A and B) further confirm
166 that stress incubation of anxiety caused the observed differences.

167

168 ***Development of different psychological components untangled in standard behavioral tests***

169 How different psychological components develop during stress incubation is still
170 unknown. From now on through the rest of the study, two questions will be addressed: (i) How
171 does a trauma-induced psychological component affect trauma-independent psychological
172 components? (ii) How does chronic anxeity, as one psychological component, increase during
173 stress incubation?

174 To answer these questions, we sequentially identified different psychological
175 components observable in mouse behaviors, demonstrated their associations in stress
176 development, determined what cause-effect system could account for the observed processes,

177 and validate the conceptual framework by testing its explanatory and predictive power on a
178 wide range of control, rescuing, and physiological conditions.

179 To explore the developmental process of different psychological components, we first
180 investigated components revealed in the light-dark box and the elevated-plus maze. In both
181 tests, key incubation features were consistently more obvious within stressor-free zones (dark
182 area and closed arms) than within stressor zones (light area and open arms). To quantitatively
183 investigate the differences between zones, we analyzed locomotor speed, as an independent
184 behavioral index of mouse position, separately in stressor and stressor-free zones (Figure 6).
185 As expected, two different behavioral patterns developed in the two zones: While speed
186 differences consistently increased in stressor-free zones (Figure 6, B and D), speed differences
187 in stressor zones only showed acute increases on Day1 (Figure 6, A and C). These results
188 suggest that different psychological components were measured in the two zones.

189 Therefore, we asked what psychological basis could account for the two behavioral
190 features separately measured in the stressor and stressor-free zones. In humans, fear is a
191 response to a known threat with a magnitude that increases with the certainty of the threat,
192 whereas anxiety is a response to uncertainty with a magnitude that increases with the
193 uncertainty of a situation [32]. Together with the presented demonstration of anxiety incubation
194 (Figures 4 and 5), we hypothesized that behavioral differences in stressor-free zones are the
195 result of anxiety reactions to uncertainty, while acute stress reactions in stressor zones are the
196 result of lasting fear responses from trauma induction. We examined mouse locomotor speed
197 in uncertain and secure environments separately, using the open field test (Figure 7, A to C; n
198 = 8 mice for each group) and the locomotor activity test (Figure 7D; n = 8 mice for each group).
199 In the open field test, mice were exposed to a dimly lit environment with a gradient of spatial
200 uncertainty from the field center (high uncertainty) to the field boundaries (low uncertainty).
201 In the locomotor activity test, mice were habituated in a dark environment with familiar cues
202 of bedding materials from their homecages indicative of less environmental stress. Compared

203 to No-scenario-isolated mice, Partner-observing mice moved faster in the center region of the
204 open field (Figure 7A), which was not observed in the periphery (Figure 7B). The difference
205 between groups increased gradually towards the center but not in the periphery (Figure 7, A
206 and B). The avoidance of spatial uncertainty by Partner-observing mice was also reflected in
207 the shorter time they spent near the center (Figure 7C, left panel) and showed a shorter latency
208 to the first rearing during the test (Figure 7C, right panel), which together suggests anxiety,
209 represented in a high tension between high uncertainty avoidance and high exploratory
210 motivation, as the causal emotional state. In contrast, Partner-observing mice moved
211 significantly slower on Day1 in the locomotor activity test and recovered on Days 7 and 28
212 (Figure 7D), suggesting an acute post-traumatic impact under low stress condition. These
213 results support the hypothesized psychological basis of anxiety and fear that account for the
214 two behavioral features with separate developments.

215 Notably, these observations of mouse spontaneous behaviors in the light-dark box test,
216 elevated plus-maze test, open field test, and locomotor activity test (Figures 6 and 7) indicated
217 a previously unexpected association between different post-traumatic stress reactions: The
218 results revealed that the two developmental patterns displayed a consistent uncertainty
219 dependence. In addition, the patterns arose together in the acute phase, but the fear pattern
220 vanished while the anxiety pattern continued to increase in the later phase. These results
221 suggest that delayed anxiety should not simply be considered an expanded, sustained response
222 of fear memory or a stress reaction induced by fear memory, because fear reactions vanish soon
223 after trauma induction. This finding refutes a general belief [1–7,18,38,39].

224

225 ***Comparison of emotionality and sociality differences suggests a unitary model***

226 Although we have demonstrated that the incubated anxiety and acute non-associative
227 fear memory developed independently in our paradigm, this indication does not distinguish a

228 unitary model from a collective model (Figure 1A): In a unitary model, the incubated anxiety
229 and acute non-associative fear memory are independently mediated by the trauma-induced state
230 of a common psychological component, and the incubated anxiety does not induce generalized
231 behavioral changes in the late phase. In a collective model, incubated anxiety and acute non-
232 associative fear memory can be independently and directly induced by the traumatic event,
233 while the incubated anxiety can also further induce generalized behavioral changes in the late
234 phase. To test both models against each other, we study the relation between emotionality,
235 specifically anxiety, and sociality in our paradigm.

236 Emotional responses simplify and speed up animal reactions to complex external cues
237 and are critical in corresponding social interactions [40]. If a sociality difference occurs and it is
238 induced by incubated anxiety, as in the case of the collective model, the growing pattern of
239 incubated anxiety should temporally precede or co-emerge with the corresponding growth
240 pattern of sociality difference. Additionally, the sociality difference should be anxiety-
241 correlated, and therefore should not occur without incubated anxiety. In the unitary model, if
242 the sociality difference develops independently after trauma induction and is independent of
243 the incubated anxiety, then the sociality difference can precede the incubated anxiety and
244 should be independent of incubated anxiety.

245 To test potential effects of anxiety on sociality, we examined mouse social motivation
246 in a two-session social test (Figure 8A): A non-social session followed by a social session (n =
247 5 mice for each group). The social stimulus was either a female or a male stranger mouse.

248 During the social session, Partner-observing mice spent less time in social approaches
249 of nose poking toward both female and male strangers, starting from Day1, and remained less
250 social compared to No-scenario-isolated mice during the post-traumatic period (Figure 8B).
251 The time they spent in the interaction zone around the social target, however, did not differ
252 significantly from that of No-scenario-isolated mice (Figure 8C). Both, Partner-observing and
253 No-scenario-isolated mice, spent only a short but similar time on nose poking during the non-

social session through the recordings on different days, with no significant difference between Partner-observing and No-scenario-isolated populations (Figure 8D), indicating that the observed difference of nose poking time was socially specific. In addition, less social vocalization was recorded during the female stranger test for Partner-observing mice (Figure 8E). These results indicated a general and chronic reduction of social interest developing after the trauma (Supplemental Video 1). This reduction of social interest differs from social avoidance due to anxiety because the social target is not avoided but just ignored [24,41].

We also analyzed locomotor speed of mice in empty sessions as an indicator of emotionality previous to social sessions, and find a notable drop of spontaneous locomotor speed starting on Days 7 and 28 (Figure 8F). Interestingly, onset of chronic reduction of social interest (starting from Day1) preceded the drop of locomotor speed. These results suggest that the changes of emotionality and sociality arise independently after trauma induction.

Relationship-dependent behaviors suggesting affectional mechanism

Two possibilities remain that could still explain a collective model: The sociality difference could be a higher-order consequence of incubated anxiety (Figures 4 to 7) or it could also be a parallel mechanism induced directly by the traumatic event. However, the following experiments reject these possibilities (Figure 9):

First, we show that affectional bonding is the key trauma-associated psychological factor that commonly mediated the development of both emotionality and sociality (Figure 10):

As Partner-observing mice experienced the traumatic event purely psychosocially, partnership between mice served as a candidate variable with which to alter the emotional impact and coping strategy [10,42,43]. Thus, we analyzed a second group of mice (Stranger-observing mice; Figure 9A) as each of them observed different stranger mice being attacked by different aggressors and stayed together with each stranger between aggressive encounters before isolation.

Stranger-observing mice did not experience any physical stress from strangers or aggressors. Two notable behavioral differences during trauma induction were observed: While tail rattling during aggressive encounters and hiding under bedding material with the partner during resting were observed in 83% (n = 39 out of 47 mice) and 100% (n = 47 out of 47 mice) Partner-observing mice (Supplemental Video 2), respectively, no such behaviors were shown by Stranger-observing mice (n = 0 out of 20 mice; n = 0 out of 20 mice). In Partner-observing mice, the frequency of tail rattles dropped progressively during aggressive encounters (Figure 10A), suggesting that it represents a rapid phasic psychological reaction during trauma induction. These results suggest that social relationship rapidly modulated emotional impact and social reactions during trauma induction. Moreover, chronic behavioral differences were not observed in Stranger-observing mice (Figure 10, B to F), which further excluded potential effects from salient, non-specific environmental manipulation (e.g. rotation through aggressors' homecages) and sensory shock (e.g. olfactory cues from urine and vocalization indicating fear) in trauma induction. Taken together, the results reveal that social relationship constitutes a critical common psychological factor that determined post-traumatic psychobehavioral development.

Considering a unitary model with social relationship as the key factor, an important question remained: Why is stress incubated, but not attenuated? As traumatic consequences were modulated by social relationship, we hypothesized that the traumatic event resulted in gradually increasing separation distress through partnership memory during social isolation. This is analog to human patients tending to recall relatively vivid memories of the past relationship after a traumatic relationship dissolution [44]. Social isolation generally disrupts mouse capacities for social recognition and social memory measured in curiosity-based behavioral tests [45,46]. We examined the persistence of social memory in a partner-revisiting test on Day28 (Figure 10G; n = 5 mice for each group). Social stimuli were the previous partner and a stranger mouse, both immobilized to allow enough social cues to be attractive, but no

305 active interaction with the focal mouse. To avoid possible influences of social cues from
306 socially defeated mice, stranger mice used to test No-scenario-isolated and Stranger-observing
307 mice were partners of Partner-observing mice. Strikingly, Partner-observing mice spent three
308 times as much time allogrooming or pushing their previous partners as did No-scenario-isolated
309 and Stranger-observing mice (Figure 10, H and Supplemental Video 3), which was opposite to
310 the lower contacts with familiar social targets in a three-chamber social novelty test where
311 curiosity to novelty dominates the behavior [46]. The preference of Partner-observing mice to
312 their previous partners, together with the findings of chronic anxiety (Figures 4 and 5) and
313 reduction of social interest (Figure 8) after separation, suggests affectional bonding as a key
314 mechanism of stress incubation in this paradigm.

315 ***Rescue of stress development by social buffering***

316 Next, we observed the development of sociality differences without the development
317 of emotionality differences when testing the necessary and sufficient conditions in our
318 paradigm (Figure 11):

319 Two important conditions in our behavioral paradigm were the increased number of
320 mice during trauma induction (visual exposure to 5 different aggressors) and the forced social
321 isolation after trauma, of which the potential effects should further be identified. We first
322 compared behavioral developments of No-scenario-isolated mice with a third control group of
323 mice (Stranger-exposed mice; Figure 9B) where the aggressor mice for trauma induction were
324 replaced by non-aggressive strangers. As the expectation (Figure 10), Stranger-exposed mice
325 did not show the developments of behavioral difference (Figure 11), confirming that social
326 aggression is necessary to induce stress developments.

327 Conceptualization of social support as a "stress buffer" have been proposed to explain
328 the positive association between responsive social resources in a small social network and
329 adverse effects of stressful events [47]. To further characterize social effects in post-traumatic

330 period, we examined the impact of social support on behavioral developments by a fourth
331 control group of mice (Partner-buffered mice; Figure 9C) as each of them was kept pair-housed
332 with its attacked partner after trauma induction. Noteworthily, developments of the differences
333 in emotionality of stress did not occur in Partner-buffered mice (Figure 9, A to C), but
334 importantly, developments that reflected their sociality showed the differences of Partner-
335 observing mice (Figure 9, D and E). This observation manifested the sufficiency of socially
336 isolated condition for anxiety incubation but not for the reduction of sociality differences. Their
337 similarity with Partner-observing mice in a longer time spent with partners extrapolates that
338 the partner revisiting test is a memory-based assay to measure social bonding in mice. The
339 observation also strengthens the position that emotionality and sociality during stress
340 incubation were separately regulated.

341 Since Partner-buffered mice experienced the same traumatic scenario as Partner-
342 observing mice, questions remain regarding the psychological mechanism for the partial rescue
343 of stress development in Partner-buffered mice. Because stress reduction through social
344 buffering depends on both social contact and social communication which can be altered by
345 emotional contagion based on different social experiences [10–12,48], and the stress-buffering
346 resources of Partner-buffered mice experienced direct trauma, we hypothesized that, in social
347 buffering, the development of emotionality difference is regulated by the social availability,
348 while the development of sociality difference is regulated by the social context. To address
349 these issues, we conducted a fifth control group of mice where each of them was kept pair-
350 housed with a stranger after trauma induction (Stranger-buffered mice; Figure 9D), and a sixth
351 control group of mice where each of them was provided with toys during social isolation after
352 trauma induction (Environment-enriched mice; Figure 9E).

353 In the Stranger-buffered paradigm, we found aggressive attacks toward defeated
354 strangers by all focal mice (n=5 out of 5) during pair-housing after trauma. Similar behavior
355 was observed when Partner-observing mice, but not their defeated partners, were group-housed

356 after trauma induction (non-recorded observation). While the observations importantly
357 illustrate partnership-specific aggressive behavior, we tested the behaviors of Stranger-
358 buffered mice only for those which were pair-housed with a non-defeated stranger. For these
359 Stranger-buffered mice, they did not displayed the developments of both emotionality and
360 sociality differences (Figure 12), with only an acute effect of positions in the light-dark box
361 test (Figure 12A).

362 Notably, although Environment-enriched mice showed similar nose poking times in the
363 female stranger test (Figure 12B) suggesting a rescue of sociality difference, they showed the
364 behavioral differences of Partner-observing mice in the light-dark box test and the non-social
365 session of female stranger test, which even had a stronger difference during the early phase
366 (Figure 12, A and C). The data corroborate the hypothesized mechanism of social buffering in
367 rescuing stress incubation and additionally emphasize the differential effects between social
368 and physical environmental enrichment.

369 ***Changes in brain connectome suggest neural substrate of unitary model***

370 Based on our behavioral results, as well as analyses of physiological conditions (Figures
371 2E and 3), we next asked if a corresponding neural framework could account for the unitary
372 model deduced from our psychobehavioral experiments. The major neuromodulatory system
373 of serotonin has long been linked to broad neural controls of physiological, sensorimotor,
374 emotional, motivational, cognitive, and social modulations [49]. Fluoxetine, as a selective
375 serotonin reuptake inhibitor, is widely used in prevalent disorders, including PTSD, regarding
376 its supposed importance on inconclusive physiological roles [50]. We investigated a seventh
377 control group of mice (FLX-treated mice; Figure 9F) as each of them was injected with
378 fluoxetine daily after trauma. Although FLX-treated mice showed less behavioral difference
379 in the early post-traumatic phase (Figure 12, A and D) and did not display a reduction of social
380 interest (Figure 12B), incubated anxiety kept developing and reached significance in the late

381 phase (Figure 12, A and D). These results exposed the limitation of a global pharmacological
382 treatment for stress incubation.

383 To further explore the physiological basis, beyond the DTI-based microstructures of
384 the brain, we investigated long-range connections of the hippocampus, as the region showing
385 the most notable differences from various measures (Figure 3). Compared with No-scenario-
386 isolated mice, among all brain regions, DTI-based fiber tracking highlighted the significant
387 increases of structural connections between the right hippocampus (CA3 and dentate gyrus)
388 and right dorsolateral entorhinal cortex (Figure 13A), an area also showed difference of its
389 mean diffusivity (Figure 3A) in Partner-observing mice. While the entorhinal cortex is the
390 main interface between the hippocampus and neocortex, we further tracked its long-range
391 connections. The right dorsolateral entorhinal cortex showed significantly increased
392 connections with the right perirhinal cortex, but had significantly decreased connections with
393 the right piriform cortex (Figure 13A). Interestingly, the piriform and perirhinal cortices are
394 the two core parahippocampal structures involve in the kindling phenomenon, the daily
395 progressive increase in response severity of both electrographic and behavioral seizure activity
396 [51,52] supposedly linked to fear conditioning in rat PTSD models [53,54]. We found a decrease of
397 the connections between the piriform and perirhinal cortices (Figure 13A). Trough further
398 tracking, we exposed a trauma-induced changes of DTI-based connectivity framework: the
399 perirhinal cortex-entorhinal cortex-hippocampus, retrosplenial cortex-hippocampus, piriform
400 cortex-amyglala, and amyglala-hypothalamus systems were centered at the anterior cingulate
401 cortex (ACC; Figure 13B), in agreement with a unitary model. These results emphasize the
402 importance of a treatment on the specific clinical target in the full mechanistic picture
403 according to a unitary model that explains, integrates, and predicts multiple mechanisms
404 underlying highly diverse behavioral consequences.

405 **Discussion**

We present a novel approach to interpret previously challenging and inconclusive behavioral development and use it to study the internal psychological development of stress incubation in laboratory mice. These results demonstrate a system-level view of experimentally disentangled components, processes, and determinants in post-traumatic stress development. While our data suggest that laboratory mice developed diverse post-traumatic reactions with comparable psychological features as observed in human, we found little support for the collective model view that a complex association among trauma-induced psychological states govern the developmental process [1–7,18,38,39] (Figure 14A). Instead, we propose a unitary model where the alteration of a single cognitive source is sufficient for triggering changes of diverse and otherwise independent psychological states (Figure 14B). Indeed, we found that the strengthening of an ACC-centered network supports the proposed unitary model for the diversity of behavioral phenotypes.

Here we summarize our results and interpretations:

Did mice display stress reactions after observing a traumatic event inflicted upon their pair-housed partners? Yes. Higher nest wall (Figure 2C), higher baseline corticosterone levels (Figure 2E), more time spent in the further end of close arms (Figure 5A), less exploration from close arms to center (Figure 5C, left panel), longer freezing time (Figure 5C, right panel), and slower locomotion (Figure 5B) in the elevated plus-maze test, more time spent in the center region (Figure 7C, left panel), and shorter latency to the first rearing (Figure 7C, right panel) in the open field test, and slower locomotion in the locomotor activity test (Figure 7D) are all classically interpreted as stress reactions. However, we also note that increased body mass (Figure 2D), more time spent in light area (Figure 4A), faster locomotion (Figure 4B), more transfers (Figure 4B, right panel), and shorter latency to the first transfer (Figure 4C, right panel) in the light-dark box test are controversial in classic readouts, an aspect we address in the next point.

431 Do standard behavioral tests of mouse anxiety completely and exclusively measure
432 mouse anxiety? No. We argue that mice display a mixture of multiple emotional aspects in
433 the standard behavioral tests with classic analyses. First, we showed that an emotional aspect
434 can yield opposite behavioral phenotypes in classic analyses of standard behavioral tests
435 (Figures 4 and 5, e.g. somatic and cognitive reactions of chronic anxiety). Second, we showed
436 that multiple emotional aspects can couple in a single behavioral test and are mixed in
437 corresponding classic analyses (Figure 6, e.g. distinct developmental patterns of fear and
438 anxiety). Classically, the emotion is inferred from specific behavioral analyses (behavior-
439 inferred emotion approach). Instead, we first considered a complete and exclusive definition
440 of the focused emotion. Then, we quantified how much of the overall behaviors matches with
441 the essential property inferred from the provided definition (emotion-inferred behavior
442 approach). Our interpretation of mouse anxiety was validated in four behavioral tests (Figures
443 6 and 7).

444 Did fear memory support the development of chronic anxiety? No. We observed the
445 continuous growth of anxiety when fear reactions had long vanished (Figures 4 to 7).

446 Did the social deficits reflect increased anxiety? No. The time course of social deficits
447 led that of increased anxiety (Figures 4, 5, and 8), and social buffering with partner mice
448 selectively rescued increased anxiety but not social deficits (Figure 11).

449 Did the trauma affect multiple behavioral aspects in parallel? No. There is a single
450 factor, affective bonding, commonly mediating diverse behavioral developments. Alternation
451 of a single social cognitive factor, social relationship, eliminated behavioral differences from
452 mice with no traumatic experience (Figures 10 and 11). Also, among all rescuing controls,
453 including social, environmental, or pharmacological approach (Figure 9, C to F), social
454 buffering with stranger mice showed the best rescuing effects on diverse behavioral aspects
455 (Figure 12).

456 Is there a neural substrate for the proposed psychological model? Yes. An
457 enhancement of an ACC-centered network was shown in DTI-based brain-wide connectome
458 analysis (Figures 3 and 13).

459 ***Detection and identification of animal emotionality***

460 We argue that classical behavioral analyses are too coarse to capture intricate emotional
461 states. The traditional approach to identify animal emotionality is to test if animals show the
462 behaviors specified by the experimental test assumed when it was designed (behavior-inferred
463 emotion approach) [55]. However, it is commonly observed that significant, robust, but
464 inconsistent behavioral outcomes are shown in different tests with the same logic and
465 assumptions [30]. Even if the results are consistent with the inferred behaviors, they can still be
466 alternatively explained [56]. The ambiguity reaches deeply into the history of widely used
467 behavioral tests and therefore have resulted in a considerable amount of inconclusive and
468 seemingly paradoxical results [57–63]. These limitations caused by circular arguments and
469 alternative interpretations should be due to the psychological and environmental factors beyond
470 the reductive condition considered in an experimental design. Classically, researchers
471 addressed the difficulties by an effort to show a proof-of-concept [9]. Here, we propose the
472 emotion-inferred behavior approach to identify animal emotionality from standard behavioral
473 tests which give inconclusive results when analyzed and interpreted in the traditional way.

474 We also introduced a simple and powerful analysis of standard behavioral tests, which
475 allowed us to discover otherwise obscured behavioral details [64]. Explaining subtle behavioral
476 differences is challenging without both richer measurements and quantitative analyses [65]. The
477 fine-scale analysis developed in our study solves this difficulty, while its utility was validated
478 by comparing it with standard analyses which in most cases prove inconclusive; that is, for the
479 analysis of stress incubation.

480 ***Biological mechanisms of mouse PTSD***

481 Behavioral paradigms of laboratory rodents that simulate PTSD were established to
482 expose the mechanistic and causal insights of long-term fear memory following acute physical
483 stress [22,23] and learned depression after repeated social defeat, either directly [66] or through
484 witnessing [19,24]. The diversity of PTSD models in mice is even highlighted by a paradigm of
485 trauma-free pharmacologically-induced memory impairments in mice, which was recognized
486 as a PTSD model and further identified the corresponding pathophysiological mechanism [14].

487 The phenomenon of stress incubation was observed and discussed in a few of these
488 animal PTSD studies. Early inhibition of PTH2R (parathyroid hormone 2 receptor)-mediated
489 TIP39 (tuberoinfundibular peptide of 39 residues) signaling in the medial amygdalar nucleus
490 was reported to enhance the increasing fear memory following a single scrambled footshock in
491 mice [20], although a system-level mechanism of stress incubation was limited by the sole
492 observation of freezing time in the study. Differentiating the effects from directly physical
493 impact, stress incubation of multiple phenotypes was more obvious in mice experiencing
494 observational stress but not in those experiencing direct attacks [19]. However, an identification
495 of post-traumatic stress incubation was challenged by significant effects of the prolonged peri-
496 traumatic stress development from the repeated trauma induction for more than a week [66].

497 Our behavioral paradigm overcomes these limitations in identifying stress incubation
498 process. With the behavioral foundation of our mouse paradigm, we propose that stress
499 incubation is a process caused by the activity-induced changes of global networks from ACC
500 after its mediation of traumatic experience. While researches on animal emotion usually
501 emphasize their ability to show human behavioral and physiological conditions (face validity),
502 to reproduce pharmacological effects in human (predictive validity), and to share the same
503 biological processes as human (construct validity) [15], a few studies have taken the possibility
504 of human-unique, animal-unique, and human-animal-sharing emotions under consideration [67].
505 We demonstrated human-animal-sharing emotions by the emotion-inferred behavior approach,

506 and showed in our paradigm that affective bonding, instead of fear memory, explains stress
507 incubation in mice.

508 ***Potential insights and applications to human PTSD***

509 Although our study focused on stress incubation in mice, the observed psychological
510 homology between mice and humans suggests that our paradigm can be used as simple model
511 of psychobehavioral development in humans. Complex developmental trajectories of human
512 PTSD symptoms were demonstrated with associated physiological and environmental
513 regulators [8], yet the combination of psychological therapy and pharmacotherapy does not
514 provide a more efficacious treatment than psychological therapy alone for PTSD development
515 [68,69]. More than leading toward a better efficacy and lower risk in conducting psychological
516 treatments, our research provides a foundation to test pharmacotherapies in a system-level view
517 that integrates multiple mechanisms underlying highly diverse behavioral consequences
518 (Figure 14). The brain heavily integrates not only external but also internal causes [70,71,80,81,72–
519 79]. Amygdala, medial prefrontal cortex, and hippocampus are the brain regions traditionally
520 focused on in human PTSD research [82], with reports emphasizing the morphology of the right
521 hippocampus [83,84]. Found on highly controlled conditions in experiments that overcome major
522 difficulties in human studies, our data in laboratory mice provide an unexpected insight of
523 PTSD development, toward brain physiology on how the potentially slow and global change
524 of brain dynamics arises from an altered dynamic in social bonding circuits through their
525 interconnected nodes (Figures 13 and 14). The efficacy of pharmacotherapies could therefore
526 be improved.

527 While much remains to be considered before clinical applications, including a better
528 connection between our mouse results and human PTSD criteria as well as a corresponding
529 study in humans, our study establishes a solid basis to uncover psychological theories for
530 therapeutic strategies [3]. Compared with the classic view of PTSD development as a process of
531 complex associations [85], we propose to consider human PTSD development as a relatively

532 simple process with a unitary origin. While the core factor in a unitary model of human PTSD
533 is not necessarily social bonding, we suggest a special focus on affective bonding as the core
534 factor for patient diagnosed with witnessing PTSD.

535 We expect that behavioral signs of PTSD development could also be detected in
536 humans already shortly after the traumatic event. The fine-scale behavioral analyses we
537 introduced here provides a simple, non-invasive analytic tool to capture informative behavioral
538 details and is not limited to laboratory animals. It opens a new window for early detection and
539 prediction with the potential to prevent a development into PTSD.

540

541 **Materials and Methods:**

542 ***Study design***

543 *Sample size.* No statistical methods were used to predetermine sample sizes. Animal numbers
544 were determined based on previous studies [9,86].

545 *Rules for stopping data collection.* Partner mice were expected to get minor injuries from
546 aggressor mice during aggressive encounters, which normally should be through attack bites
547 on the dorsal side of posterior trunk [86]. The aggressive encounter and all further experiments
548 were terminated once (i) the partner mouse showed severe bleeding or ataxia, or (ii) the
549 aggressor mice showed abnormal attack bites on any other body part. Partner mice that reached
550 the criteria (i) were euthanized. Aggressor mice that reached the criteria (ii) were terminated
551 its usage in any further experiments. If any aggressive sign (sideways threat, tail rattle, pursuit,
552 and attack bite) was shown by the partner mouse, all further experiments with the partner mouse,
553 aggressor mouse, and observer mouse were terminated.

554 *Data inclusion/exclusion criteria.* No data were excluded.

555 *Outliers.* No outliers were defined.

556 *Selection of endpoints.* The endpoints were prospectively selected. The criteria were approved
557 by the Institutional Animal Care and Use Committee (IACUC) in the animal facility at the
558 Okinawa Institute of Science and Technology (OIST) Graduate University, accredited by the
559 Association for Assessment and Accreditation of Laboratory Animal Care (AAALAC).

560 *Replicates.* All behavioral tests were conducted in quintuplicate to octuplicate sampling
561 replicates. All behavioral tests were conducted in single experimental cohorts. All other
562 records were conducted in quadruplicate to septuplicate experimental cohorts.

563 *Research objectives.* The goal of this work is to identify diverse psychological aspects,
564 temporal patterns, and associations of behavioral development in mice after a single trauma
565 induction. Pre-specified hypotheses stated that (i) internal psychological development is
566 already represented in behavioral details during early post-traumatic phase, while (ii) an
567 association among trauma-induced states such as fear memory, increased anxiety, and social
568 withdrawal explains PTSD-like behavioral development. Our data support the first pre-
569 specified hypothesis, but not the second. All other hypotheses were suggested after initiation
570 of the data analyses.

571 *Research subjects or units of investigation.* 8-week-old male C57BL/6J mice, 16-week-old
572 female C57BL/6J mice, and 20-week-old or older male Slc:ICR mice were used.

573 *Experimental design.* We approached the research goal by developing a novel mouse model
574 of psychosocial trauma under highly controlled conditions (psychosocial manipulations,
575 subjective experiences, and genetic background) and by applying fine-scale analysis to
576 standard behavioral tests. To induce acute witnessing trauma, a pair-housed mouse observed
577 how its partner got bullied by a larger, aggressive mouse on the day of trauma induction. After
578 this trauma, the observer mouse was isolated and developed behavioral differences compared
579 to control mice in the ensuing weeks. The control groups included (i) mice isolated without
580 experiencing trauma induction, (ii) mice isolated after observing how a stranger mouse got

581 bullied by a larger, aggressive mouse, (iii) mice isolated after exposed to a non-aggressive
582 stranger mouse, (iv) mice which were pair-housed with their defeat partners after observing
583 how its partner got bullied by a larger, aggressive mouse, (v) mice which were pair-housed
584 with strangers after observing how its partner got bullied by a larger, aggressive mouse, (vi)
585 mice isolated with their environment enriched, and (vii) mice isolated with daily injections of
586 fluoxetine. The behavioral tests included the light-dark box test, elevated plus-maze test, open
587 field test, locomotor activity test, active social contact test to a female stranger, active social
588 contact test to a male stranger, and partner-revisiting test. The non-behavioral tests included
589 the body mass measurement, nest wall height measurement, baseline corticosterone
590 concentration test, and ex vivo diffusion tensor imaging.

591 *Randomization.* Mice were from different litters. Mice were randomly paired. A focal mouse
592 was randomly selected from each pair of mice. Mice were randomly allocated into
593 experimental groups. Testing order among groups was counterbalanced. Strangers and
594 aggressors were randomly assigned.

595 *Blinding.* The investigator was blinded to behavioral outcomes but not to group allocation
596 during data collection and/or analysis.

597 ***Overview***

598 All experimental procedures were approved by IACUC in the animal facility at the
599 OIST Graduate University, accredited by AAALAC. In total, 467 male C57BL/6J mice (CLEA
600 Japan, Inc.), 49 female C57BL/6J mice (CLEA Japan, Inc.), and 33 male Slc:ICR mice (Japan
601 SLC, Inc.; retired from used for breeding) were used in this study. In CLEA Japan, nursing
602 females were individually housed (CL-0103-2; 165×234×118 mm), while pups were separated
603 on P21 according to gender and housed ≤15 mice per cage (CL-0104-2; 206×317×125 mm).
604 Pups were re-arranged on P28 according to their weights and housed ≤13 mice per cage (CL-
605 0104-2). Mice were shipped in boxes each with 10 – 30 mice to the OIST Animal Facility. In

606 the OIST Animal Facility, mice were housed in 380×180×160-mm transparent holding cages
607 (Sealsafe Plus Mouse DGM - Digital Ready IVC; Tecniplast Inc., Quebec, Canada) bedded
608 with 100% pulp (FUJ9298101; Oriental Yeast Co., Ltd., Tokyo, Japan) under a 12-hr dark/light
609 cycle (350-lux white light) at a controlled temperature of 22.7 – 22.9 ºC, humidity of 51 – 53%,
610 and differential pressure of -14 – -8 Pa with food and water available ad libitum. Circadian
611 time (CT) is defined to start at mid-light period and described in a 24-hr format, i.e. light off at
612 CT 6:00.

613 The experimenter and caretakers wore laboratory jumpsuits, lab boots, latex gloves,
614 face masks, and hair nets when handling mice and performing experiments. Handling of mice
615 during the dark cycle was done under dim red light and mice were transported in a lightproof
616 carrier within the animal facility. For mice in experimental and control groups tested on the
617 same dates, the testing order was alternated. Surfaces of experimental apparatuses were wiped
618 with 70% ethanol in water and dry paper tissues after testing each mouse to remove olfactory
619 cues. Each mouse was only used for one behavioral test (in total 4 records with intervals of 6
620 – 21 days) to avoid confounded results due to cross-testing and to minimize measurement
621 effects on its psychological development [41].

622 ***Pre-traumatic period (Day-21 to Day0)***

623 To establish partnerships between mice, a male C57BL/6J mouse (focal mouse; 8 weeks)
624 was pair-housed with another male C57BL/6J mouse (partner mouse; 8 weeks) for 3 weeks
625 (Day-21 to Day0, with trauma induction on Day0). The partner was initially marked by ear
626 punching. The holding cage was replaced once per week, with the last change 3 days before
627 the traumatic event (Day-3).

628 To establish the territory of an aggressor mouse in its homecage, an Slc:ICR mouse
629 (aggressor mouse; ≥20 weeks) was pair-housed with a female C57BL/6J mouse (female mouse;

630 16 weeks) for 3 weeks (Day-21 to Day0). The holding cage was replaced with a clean one
631 once a week, with the last change one week before the traumatic event (Day-7).

632 Aggression level of aggressors was screened on Days -5, -3, -1 through intruder
633 encounters [87] toward different screening mice to determine appropriate aggressors to be used
634 for trauma induction on Day0. Aggression screening was carried out in the behavior testing
635 room at 22.4 – 23.0 ºC, 53 – 58% humidity, -4 – -3 Pa differential pressure, and 57.1 dB(C)
636 ambient noise level during the light period (CT 4:00 – 6:00) with 350-lux white light. After the
637 female and pups with the aggressor were taken out of their homecage and kept in a clean
638 holding cage in the behavior testing room, a 3-min aggression screening was started after a
639 male C57BL/6J mouse (screening mouse; 10 weeks) was brought into the homecage of the
640 aggressor, followed by covering the cage with a transparent acrylic lid. During screening, the
641 aggressor freely interacted with the screening mouse. The aggressor was brought back to the
642 holding room after the screening mouse was taken away from the aggressor's homecage and
643 the female and pups were brought back to its homecage right after screening. Aggressors were
644 selected for trauma induction on Day0 if they showed biting attacks on all of these screening
645 days and the latencies to the initial bites on Day-3 and Day-1 were less than 20 s.

646 ***Trauma induction (Day0)***

647 The following experimental assay emotionally introduced an acute traumatic
648 experience in mice through a social process. The setup was the aggressor's homecage, divided
649 into an 80×180-mm auditorium zone and a 300×180-mm battle arena by the insertion of a
650 stainless-steel mash with 8×8-mm lattices. The cage was covered with a transparent acrylic
651 lid. The behavioral procedure was carried out in the behavior testing room during CT 4:00 –
652 6:00, with 3 – 5 experiments done in parallel.

653 After the female and pups with the aggressor were taken out of their homecage, a
654 divider was inserted into the aggressor's homecage, allowing the aggressor to freely behave in

655 the battle arena, but not to enter the auditorium zone. A 5-min aggression encounter session
656 started after the focal mouse was brought to the auditorium zone and its partner to the battle
657 arena. Tail rattling counts of the focal mouse during aggressive encounter were recorded by
658 experimenter. The aggressive encounter session was followed by a 5-min stress infiltration
659 session, in which the partner was brought to the focal mouse in the auditorium zone, while the
660 aggressor remained in the battle arena. Right after the stress infiltration session, both focal
661 mouse and its partner were brought back to their homecage in the behavior testing room for a
662 10-min resting period. The procedure was repeated 5 times with different aggressors. During
663 each resting session, the aggressor stayed in its homecage without the divider before its next
664 intruder encounter. Each aggressor had 3 – 5 encounters with resting periods of 10 – 30 min.
665 After the 5th aggression encounter session, the focal mouse was placed back in its homecage
666 where the nest had been razed, and brought back to the holding room. Partners from different
667 pairs were brought to a new holding cage and housed in groups of 3 – 5 per cage. Right after
668 the last intruder encounter for each aggressor, the female and pups were brought back to the
669 homecage and returned to the holding room together with the aggressor.

670 ***Post-traumatic period (Day0 to Day28)***

671 To investigate the behavior of focal mice after trauma induction (now called Partner-
672 observing mice, Figure 2A), they were housed individually for 4 weeks after the procedure
673 (Day0 to Day28). No environmental enrichment was provided, except to the Environment-
674 enriched mice, and the holding cage was not changed during social isolation.

675 ***Control experiments***

676 To differentiate behavioral consequences of the emotionally traumatic experience from
677 consequences of social isolation, a control group of mice had their partners taken away and
678 their nests razed during body weighing on Day0 without trauma induction (No-scenario-
679 isolated mice, Figure 2B).

680 To test the influence of social relationship on the emotionally traumatic experience, a
681 control group of mice witnessed the traumatic events toward stranger mice of the same strain,
682 gender, and age instead (Stranger-observing mice, Figure 9A). In each iteration of the
683 aggression encounter, stress infiltration, and resting period, a different stranger mouse was
684 presented.

685 To identify the impacts of aggression during trauma induction, a control group of mice
686 experienced exposure to strangers of the same strain, gender, and age, instead of the aggressor
687 mice for trauma induction (Stranger-exposed mice, Figure 9B).

688 To examine the potential reversal effects of social support on the emotionally traumatic
689 experience, a control group of mice was kept pair-housed with their attacked partners after
690 trauma induction (Partner-buffered mice, Figure 9C).

691 To further test the critical component of social relationship in the potential social
692 support reversal, a control group of mice was kept pair-housed but with a stranger mouse after
693 trauma induction (Stranger-buffered mice, Figure 9D).

694 To characterize potential reversal effects through environmental factors besides social
695 factors, a control group of mice was housed individually with environmental enrichment,
696 provided with a pair of InnoDome™ and InnoWheel™ (Bio-Serv, Inc., Flemington, NJ, USA)
697 and a Gummy Bone (Petite, Green; Bio-Serv, Inc.), after trauma induction (Environment-
698 enriched mice, Figure 9E).

699 To demonstrate predictive validity of potential treatment on stress by an antidepressant,
700 a control group of mice was intraperitoneally injected with fluoxetine (2 μl/g of 10 mg/ml
701 fluoxetine hydrochloride dissolved in saline, i.e. 20 mg/kg; F132-50MG; Sigma-Aldrich, Inc.,
702 Saint Louis, MO, USA) once per day at CT 1:00 – 2:00 after trauma induction (FLX-treated
703 mice, Figure 9F).

704 ***Body mass and nest wall height***

In the holding room, body masses of all individuals were recorded on Days -7, 0, 1, 7, 28, while the heights of nest walls built by each individual were recorded on Days 1, 7, 28. The height of the nest wall was measured with 5-mm resolution using a transparent acrylic ruler, while the mouse was weighed with 10-mg resolution on a balance. Mice were placed back in their homecages right after recording.

Light-dark box test

The light-dark box test is an experimental assay to measure anxiety in rodents [88], designed to evaluate their natural aversion to brightly lit areas against their temptation to explore. The light-dark box setup consisted of two connected 200×200×250-mm non-transparent PVC boxes, separated by a wall with a 50×30-mm door. The boxes were covered with lids with white and infrared LED light illumination for the light and dark areas, respectively, and CCD cameras in the centers (4-chamber system; O'Hara & Co., Ltd., Tokyo, Japan). The floors of the boxes were white, while the walls of the boxes were white for the light area and black for the dark area. Uniform illumination in the light area was 550 lux. Behavioral tests were carried out on Days -7, 1, 7, and 28 in the behavior testing room at 22.7 – 23.0 ºC, 51 – 54% humidity, -11 – -9 Pa differential pressure, and 53.6 dB(C) ambient noise level during dark period (CT 6:00 – 8:00).

After habituation for 10 min individually in the homecage in the behavior testing room in darkness, the focal mouse was transferred to the dark area through a 50×50-mm side door. A 5-min behavior record was started right after the side door of dark area was closed and the door between light and dark areas was opened. Locomotion was recorded 2-dimensionally at 15 Hz from top-view with CCD video cameras. Right after recording, the mouse was returned to its homecage, and brought back to the holding room.

Elevated plus-maze test

729 The elevated plus-maze test is an experimental assay to measure anxiety in rodents [89],
730 designed to evaluate their natural fear of falling and exposure against their temptation to
731 explore. The elevated plus-maze setup consisted of a gray PVC platform raised 500 mm above
732 the ground (single maze system; O'Hara & Co., Ltd.). The platform was composed of a 50×50-
733 mm square central platform, two opposing 50×250-mm open arms, and two opposing 50×250-
734 mm closed arms with 150-mm semi-transparent walls. Each of the two open arms emanated at
735 90° to each of the two closed arms, and vice versa. The apparatus was installed in a soundproof
736 box with white fluorescent lamp illumination (20 lux) and ventilators. Behavioral tests were
737 carried out on Days -7, 1, 7, 28 in the behavior testing room at 22.8 – 23.0 ºC, 53 – 56%
738 humidity, -13 – -11 Pa differential pressure, and 52.1 dB(C) ambient noise level during dark
739 period (CT 8:00 – 10:00).

740 After habituation for 10 min individually in the homecage in the behavior testing room
741 in darkness, the focal mouse was brought to the central platform of the elevated plus-maze,
742 facing the open arm on the opposite side from the door of the soundproof box. A 5-min
743 behavior recording was started right after the door of the soundproof box was closed.
744 Locomotion was recorded 2-dimensionally at 15 Hz from top-view with a CCD video camera
745 installed above the center of the central platform. Delineated entrances to open and closed
746 arms were defined at 50 mm from the center of the central platform. Right after recording, the
747 mouse was placed back in its homecage, and brought back to the holding room.

748 ***Open field test***

749 The open field test is an experimental assay to measure anxiety in rodents [90], designed
750 to evaluate their spontaneous activity under a gradient of spatial uncertainty (high in the field
751 center and low along the walls and at the corners of the field). The open field setup consisted
752 of a 400×400×300-mm non-transparent gray PVC box with no cover, installed in a soundproof
753 box with white LED light illumination and ventilators (2-chamber system; O'Hara & Co., Ltd.).
754 Behavioral tests were carried out on Days -7, 1, 7, 28 in the behavior testing room at 22.8 –

755 23.0 ºC, 53 – 56% humidity, -13 – -11 Pa differential pressure, and 56.7 dB(C) ambient noise
756 level during dark period (CT 8:00 – 10:00).

757 After habituation for 10 min individually in the homecage in the behavior testing room
758 in darkness, the focal mouse was brought to the center of the open field arena under 20-lux
759 uniform illumination, facing the wall on the opposite side from the door of the soundproof box.
760 A 5-min behavior recording was started right after the door of the soundproof box was closed.
761 Locomotion was recorded 2-dimensionally at 15 Hz from top-view with a CCD video camera
762 installed above the center of the open field arena. Vertical activity of exploratory rearing
763 behavior was recorded by the blocking of invisible infrared beams created and detected by
764 photocell emitters and receptors, respectively, positioned 60 mm high on the walls of the open
765 field box. A delineated center region was defined as the central 220×220 mm area. Right after
766 recording, the mouse was placed back in its homecage, and returned to the holding room.

767 ***Locomotor activity test***

768 The locomotor activity test is an experimental assay to measure spontaneous activity of
769 rodents in an environment without an experimentally designed stressor. The locomotor activity
770 setup consisted of a 200×200×250 mm non-transparent covered PVC box with infrared LED
771 illumination and a CCD camera in the center (the dark area of the light-dark box setup, while
772 the door between the light and dark areas was closed and fixed). The floor of the box was
773 embedded with bedding material from the homecage of the focal mouse, while the walls of the
774 box were black. Behavioral test was carried out on Days -7, 1, 7, 28 in the behavior testing
775 room at 22.7 – 23.0 ºC, 51 – 54% humidity, -11 – -9 Pa differential pressure, and 53.6 dB(C)
776 ambient noise level during dark period (CT 6:00 – 8:00).

777 After habituation for 30 min individually in the behavior testing box, a 1-hr behavior
778 recording was started. The behavior testing box was not covered completely in order to allow
779 air circulation. Locomotion was recorded 2-dimensionally at 15 Hz from top-view with the

780 CCD video camera. Right after recording, the mouse was returned to its homecage, and
781 brought back to the holding room.

782 ***Active social contact test***

783 The active social contact test (also known as "social interaction test", but to be
784 distinguished with the one-session test using an open field with a social target freely behaving
785 in the field [91] or the one-session test placing a social target-containing cylinder into the center
786 of the testing subject's homecage for social instigation [92]) is a 2-session experimental assay to
787 measure social motivation in rodents [93]. The setup consists of a 400×400×300-mm non-
788 transparent gray PVC box with no cover, installed in a soundproof box with 20-lux white LED
789 illumination and ventilators. A 60×100×300-mm stainless-steel chamber with wire grid sides
790 was placed in the center of the wall on the opposite side from the door of the soundproof box.
791 The wire grid had 8×8 mm lattices at a height of 10 – 60 mm from the bottom. An ultrasound
792 microphone (CM16/CMPA; Avisoft Bioacoustics, Glienicke, Germany) with an acoustic
793 recording system (UltraSoundGate; Avisoft Bioacoustics) was hung outside the chamber, 100
794 mm above the ground. Behavioral tests were carried out on Days -7, 1, 7, 28 in the behavior
795 testing room at 22.8 – 23.0 ºC, 53 – 56% humidity, -13 – -11 Pa differential pressure, and 56.7
796 dB(C) ambient noise level during dark period (CT 8:00 – 10:00).

797 The social target used for active social contact tests was either a male or a female
798 C57BL/6J mouse (18 weeks), pair-housed with a partner of the same strain, gender, and age
799 for more than 2 weeks before the tests. The social target was adapted to the experimental
800 protocol one day before the tests in the behavior testing room during dark period (CT 8:00 –
801 9:00): After habituation for 5 min individually in the homecage in the soundproof box under
802 20-lux uniform illumination, the social target was brought into the chamber in the open field
803 arena under 20 lux uniform illumination. A male C57BL/6J mouse (11–16 weeks; from
804 partners of No-scenario-isolated mice in previous experiment) was then brought to the open
805 field arena for a 2.5-min spontaneous exploration and interaction with the social target. The

806 social target was then brought back to its homecage in the soundproof box under 20-lux
807 uniform light for a 5-min rest. The social interaction procedure was repeated with a different
808 male C57BL/6J mouse right afterward. After the social target had interacted with 4 different
809 mice, it was returned to its homecage and brought back to the holding room.

810 On testing days, after 10-min habituation individually in its homecage in the behavior
811 testing room in darkness, the first session of the active social contact test started by placing the
812 focal mouse at the center of the open field arena under 20-lux uniform light, facing the empty
813 chamber. A 2.5-min behavior recording started right after the door of the soundproof box was
814 closed. Locomotion was recorded 2-dimensionally at 15 Hz from top-view with a CCD video
815 camera installed above the center of the open field arena. Ultrasonic vocalization was recorded
816 at 250 kHz. In the second session of the active social contact test, which followed the first
817 session, the social target was brought into the chamber. Another 2.5-min behavior recording
818 started as soon as the door of the soundproof box was closed. Right afterward, the focal mouse
819 was returned to its homecage and brought back to the holding room.

820 The focal mouse experienced active social contact tests with different social targets on
821 different recording days (Days -7, 1, 7, 28), while different focal mice were tested with the
822 same social target on the same recording day (5 – 10 records). The social target remained in
823 its homecage in a soundproof box under 20-lux uniform illumination before and between each
824 test. A delineated interaction zone was taken as the region within 80 mm of the edges of the
825 chamber. Social approaches of the focal mouse poking its nose toward the social target were
826 recorded manually using the event recording software, tanaMove ver0.09 (http://www.mgrl-
827 lab.jp/tanaMove.html).

828 ***Partner-revisiting test***

829 The partner-revisiting test is a memory-based experimental assay to measure social
830 bonding in rodents (sharing similar concept of "familiar v.s. novel social target recognition",

831 but to be distinguished with the three-chamber paradigm test [94]). The partner-revisiting setup
832 was the uncovered homecage of the focal mouse, installed in a soundproof box with white LED
833 illumination and ventilators (O'Hara & Co., Ltd., Tokyo, Japan). The long sides of the
834 homecage were parallel to the door of soundproof box. The partner-revisiting test was carried
835 out on Day28 in the behavior testing room at 22.8 – 23.0 ºC, 53 – 56% humidity, -13 – -11 Pa
836 differential pressure, and 56.7 dB(C) ambient noise level during light period (CT 4:00 – 6:00)
837 with 350-lux light intensity.

838 The previously separated partner of the focal mouse, being a social target in the test,
839 was initially sedated with 3%v/v isoflurane in oxygen, and then anesthetized by intraperitoneal
840 (i.p.) injection of a mixture of medetomidine (domitor, 3%v/v in saline, 0.3 mg/kg), midazolam
841 (dormicum, 8%v/v in saline, 4 mg/kg), and butorphanol (vetorphale, 10%v/v in saline,5 mg/kg).
842 Also, a stranger mouse (15 weeks; a separated partner of a Partner-observing or Buffered mouse
843 for testing a No-scenario-isolated, Stranger-observing, or Stranger-exposed mouse, and *vice*
844 *versa*) was anesthetized as an alternative social target. Both anesthetized mice were kept on a
845 heating pad at 34ºC (B00O5X4LQ2; GEX Co., Ltd., Osaka, Japan) to maintain their body
846 temperatures before the test.

847 The focal mouse was brought to a clean, uncovered holding cage in the soundproof box
848 under 50-lux uniform illumination for 5-min habituation, while its homecage was placed in
849 another soundproof box under 50-lux uniform light. During habituation of the focal mouse,
850 the anesthetized social targets were injected with atipamezole hydrochloride (antisedan; 6%v/v
851 in saline for 0.3 mg/kg, i.p.) to induce recovery from anesthesia. During the waking-up period,
852 the social targets were still immobilized and not able to actively interact with the focal mouse
853 during the following recording, but showed enough social cues to be attractive for the focal
854 mouse. The immobilized social targets were then placed in the homecage of the focal mouse
855 with their nose pointing toward the center of the short side of the wall (10 mm of nose-to-wall
856 distance) with their bellies facing the door of the soundproof box. After habituation, the focal

857 mouse was brought to the center of its homecage, facing the long side of the homecage wall on
858 the opposite side from the door of soundproof box. A 10-min behavior record started right
859 after the door of the soundproof box was closed. Locomotion was recorded 2-dimensionally
860 at 15 Hz from top-view with a CCD video camera installed above the center of the homecage.
861 Right after recording, social targets were taken out of the focal mouse's homecage and the focal
862 mouse was brought back to the holding room.

863 Social contacts including sniffing, allogrooming, and pushing of the focal mouse
864 toward each of the social targets were recorded manually using the event recording software,
865 tanaMove ver0.09 (http://www.mgrl-lab.jp/tanaMove.html).

866 ***Baseline plasma corticosterone concentration test***

867 The baseline plasma corticosterone (CORT) concentration test is a competitive-
868 inhibition enzyme-linked immunosorbent assay (ELISA) to measure physiological stress level
869 in rodents, designed to quantitatively determinate CORT concentrations in blood plasma. The
870 sample collection was carried out on Days -7, 1, 7, 28 in the behavior testing room at 22.4 –
871 23.0 ºC, 53 – 58% humidity, -4 – -3 Pa differential pressure, and 57.1 dB(C) ambient noise
872 level during CT 4:00 – 6:00 with 350-lux white light.

873 After habituation for 30 min individually in the homecage in the behavior testing room,
874 the mouse was initially sedated with 3%v/v isoflurane in oxygen. Six drops of blood from the
875 facial vein pricked by a 18G needle were collected in a EDTA-lined tube [K2 EDTA (K2E)
876 Plus Blood Collection Tubes, BD Vacutainer; Becton, Dickinson and Company (BD), Franklin
877 Lakes, NJ, USA] and kept on ice. Right after collection, the mouse was returned to its
878 homecage, and brought back to the holding room. Whole blood samples were then centrifuged
879 (MX-300; Tomy Seiko Co., Ltd., Tokyo, Japan) at 3,000 rpm for 15 min at 4°C. Plasma
880 supernatant was decanted and kept at -80°C until the measurement on Day 29.

881 CORT concentrations in blood plasma were tested with Mouse Corticosterone (CORT)
882 ELISA Kit (MBS703441, 96-Strip-Wells; MyBioSource, Inc., San Diego, USA; stored at 4°C
883 before use) on Day 29. All reagents [assay plate (96 wells, pre-coated with goat-anti-rabbit
884 antibody), standards (0, 0.1, 0.4, 1.6, 5, and 20 ng/ml of CORT), rabbit-anti-CORT antibody,
885 HRP-conjugated CORT, concentrated wash buffer (20x phosphate-buffered saline (PBS)),
886 3,3',5,5'-tetramethylbenzidine (TMB) color developing agent (substrates A and B), and TMB
887 stop solution] and samples were brought to room temperature for 30 min before use. Collected
888 plasma samples after thawing were centrifuged again (MX-300; Tomy Seiko Co.) at 3,000 rpm
889 for 15 min at 4°C. 20 µl of standard or sample was added per well, assayed in duplicate, with
890 blank wells set without any solution. After 20 µl of HRP-conjugated CORT was added to each
891 well except to the blank wells, 20 µl of rabbit-anti-CORT antibody was added to each well and
892 mixed. After incubation for 1 hour at 37°C, each well was aspirated and washed, repeated for
893 3 times, by filling each well with 200 µl of wash buffer (diluted to 1x PBS) using a squirt bottle,
894 standing for 10 s, and completely removing liquid at each step. After the last wash and the
895 removal of any remaining wash buffer by decanting, the plate was inverted and blotted against
896 clean paper towels. After TMB color developing agent (20 µl of substrate A and 20 µl of
897 substrate B) was added to each well, mixed, and incubated for 15 min at 37°C in dark, 20µl of
898 TMB stop solution was added to each well and mixed by gently tapping the plate. The optical
899 density (O.D.) of each well was determined, within 10 min, using a microplate reader
900 (Multiskan GO; Thermo Fisher Scientific, Inc., Waltham, MA, USA) measuring absorbance at
901 450 nm, with correction wavelength set at 600–630 nm.

902 CORT concentrations were calculated from the O.D. results using custom scripts
903 written in MATLAB R2015b (MathWorks). The duplicate O.D. readings for each standard and
904 sample was averaged and subtracted the average O.D. of the blanks, $X = \langle O.D. \rangle -$
905 $\langle O.D. \rangle_{blank}$. A standard curve was determined by a four parameter logistic (4PL) regression

906 fitting the equation $\rho_{CORT}(X_{standard}) = d + \frac{a-d}{1+(\frac{X_{standard}}{c})^b}$, where ρ_{CORT} is the CORT

907 concentration, a is the minimum asymptote, b is the Hill's slope, c is the inflection point, and

908 d is the maximum asymptote. CORT concentrations of the samples were calculated from the

909 fitted 4PL equation with respected to X_{sample}.

910 ***Ex vivo diffusion tensor imaging***

911 *Ex vivo* diffusion tensor imaging (DTI) is a magnetic resonance imaging (MRI)

912 technique to determinate structural information about tissues [95], designed to measure the

913 restricted diffusion of water in tissue. The sample collection was carried out on Day 28 in the

914 necropsy room at 22.4 - 22.5 ºC, 53 - 54 % humidity, and 10 - 12 Pa differential pressure during

915 CT 4:00 - 6:00 with 750-lux white light.

916 After mice were brought individually in their homecages to the necropsy room, they

917 were initially sedated with 3%v/v isoflurane in oxygen, then deeply anaesthetized with a

918 ketamine-xylazine mixture (>30 µl/g body weight of 100 mg/ml ketamine and 20 mg/ml

919 xylazine), and perfused transcardially. The perfusates, in a two-step procedure, were (i) 20 ml

920 of ice cold 1x phosphate-buffered saline (PBS), and (ii) 20 ml of ice cold 4% paraformaldehyde,

921 0.2% sodium meta-periodate, and 1.4% lysine in PBS. Mouse skull including the brain was

922 removed and stored in the perfusate (ii) at 4 ºC for 2 weeks. Each skull with the brain was then

923 transferred into 2 mM gadolinium with diethylenetriaminepentaacetic acid (Gd-DTPA) and

924 0.5% azide in PBS for 2 weeks.

925 Isolated fixed brains within the skulls were positioned in an acrylic tube filled with

926 fluorinert (Sumitomo 3M Ltd., Tokyo, Japan) to minimize the signal intensity attributable to

927 the medium surrounding the brain during MRI scanning. All MRI was performed with an 11.7-

928 T MRI system (BioSpec 117/11; Bruker Biospec, Ettlingen, Germany) using ParaVision 6.0.1

929 software (Bruker Biospec, Ettlingen, Germany) for data acquisition. The inner diameter of the

930 integrated transmitting and receiving coil (Bruker Biospec, Ettlingen, Germany) was 35 mm

for the ex vivo MRI. DTI data were acquired by using a 3-D diffusion-weighted spin-echo imaging sequence, with repetition time (TR) = 267 ms, echo time (TE) = 18.5 ms, b-value = 2,000 s/mm2, and 30 non-collinear directions. Five T2-weighted measurements were acquired together with DTI, for one every 6 diffusion measurements. The acquisition matrix was 216×216×168 over a 27.0×27.0×21.0 mm3 field of view, resulting in a native isotropic image resolution of 125 μm. Total acquisition time was 96 hr.

MRI data was processed using custom scripts written in MATLAB R2015b (MathWorks). All 30 DTI and 5 T2 3-D images were masked by thresholding at the half of mean values of diffusion weights for each voxel and omiting clusters smaller than 10 voxels. After diffusion tensor of each voxel was estimated by solving the Stejskal-Tanner equation through linear regression [96], the 3 eigenvalues (λ_1, λ_2, and λ_3) with respect to the 3 axes of the diffusion ellipsoid (the longest, middle, and shortest axes, respectively) were calculated by eigenvalue decomposition of the diffusion tensor. Four focused DTI-based measures [97] are the mean diffusivity (MD) that represents membrane density

$$MD = \langle \lambda \rangle = \frac{\lambda_1 + \lambda_2 + \lambda_3}{3},$$

axial diffusivity (AD) that represents neurite organization

$$AD = \lambda_1 ,$$

radial diffusivity (RD) that represents myelination

$$MD = \frac{\lambda_2 + \lambda_3}{2},$$

and fractional anisotropy (FA) that represents average microstructural integrity

$$FA = \sqrt{\frac{3 \times [(\lambda_1 - \langle \lambda \rangle)^2 + (\lambda_2 - \langle \lambda \rangle)^2 + (\lambda_3 - \langle \lambda \rangle)^2]}{2 \times \left({\lambda_1}^2 + {\lambda_2}^2 + {\lambda_3}^2\right)}}.$$

952 After the registration of these 3-D DTI-based brain maps to a template brain atlas
953 (DSURQE Atlas; https://wiki.mouseimaging.ca/display/MICePub/Mouse+Brain+Atlases),
954 mean values of these DTI-based quantities were identified in a total of 244 brain regions ($)
955 for each individual. Based on the FA maps, DTI-based long-range fiber tracking from a focal
956 seed region ($B) was calculated with 2 samplings, distance of forward fiber in one step = 50
957 μm, and thresholds of minimal fiber length = 750 μm, maximal fiber length = 75,000 μm,
958 maximal fiber deviation angle = 57.3º, and minimal FA for keeping tracking = 0.4.

959 ***Video image process***

960 Video image data was processed using custom scripts written in MATLAB R2015b
961 (MathWorks). Each video frame from a recorded AVI video file was read as a 2-dimensional
962 matrix with an 8-bit gray scale. Each of these matrices was then divided by a background
963 matrix read from a TIF image file of the background taken before bringing the test mouse to
964 the setup. The centroid of the area with non-one values in each matrix ratio was taken as the
965 position of the mouse at this specific time point. Speed was calculated as the distance between
966 temporally adjacent positions multiplied by 15 (15-Hz recording). Freezing periods were
967 sorted out if the area of the mouse body between temporally adjacent frames was less than 20
968 mm^2.

969 ***Audio signal process***

970 Audio signal data was processed with custom scripts written in MATLAB R2015b
971 (MathWorks). Each recorded WAV audio file was read and transformed into a spectrogram
972 using fast Fourier transform with non-overlapping 0.4-ms time windows. To identify the time
973 segments with ultrasonic vocalization signals, recordings were thresholded at a power spectral
974 density (PSD) ≥-75 dB/Hz, and time segments with averaged PSD between 0–50 kHz higher
975 than that between 50–120 kHz were removed. The duration of remaining time segments was
976 calculated.

977 ***Statistical analysis***

978 Numerical data were analyzed with custom scripts written in MATLAB R2015b
979 (MathWorks). Statistical significance of the difference between 2 mean values was estimated
980 with two-tailed, two-sample Student's t-test, except of DTI quantities which were estimated
981 with one-tailed, two-sample Student's t-test. Statistical significance of the difference between
982 2 median values (vocalization analysis; Figure 8F) was estimated using one-tailed Mann–
983 Whitney U test.

984 To capture fine-scale behavioral details of location within the light-dark box and the
985 elevated plus-maze (Figures 4 and 5), we computed T(x), the cumulative probability of finding
986 position ≤x, for each individual (light traces) for all measured locations (a collection of
987 locations from all mice for the statistics). We then show the average across the control group
988 (bold blue trace) and the Partner-observing group (bold red trace). We compared the averages
989 of each group with a two-tailed, two-sample Student's t-test and plot the resulting p-values,
990 presented as -log(p), the negative logarithm of p-values. We also show the box plot (the
991 minimum, lower quartile, median, upper quartile, and maximum) of -log(p) values collapsed
992 across all measured locations. To capture the fine- scale behavioral details of speed, we
993 followed a similar procedure as above, but with U(v), the cumulative distribution function of
994 finding speed ≤v.

995 To evaluate the uncertainty of the percentage for each tail rattle count (Figure 10A), we
996 created 10,000 bootstrapped data sets where each sample was randomly picked with
997 replacement from the original data set. Each bootstrapped data set had the same sample size as
998 the original data set. The standard error was taken as the standard deviation of the bootstrapped
999 percentages for a tail rattle count. A similar procedure was carried out to evaluate the standard
1000 error of mean for the percentage of time spent in each behavior in the partner-revisiting test
1001 (Figures 10H and 11E), where each sample of the bootstrapped data sets was a set of the

percentages of the three classified behaviors (partner concern, stranger concern, and non-social activity/sniffing at social targets) from a mouse record. Standard errors of means for other results were estimated with the formula $\sigma/\sqrt{n}$, where σ is the sample standard deviation and n is the sample size.

Acknowledgments: We thank Tsuyoshi Koide (NIG, Japan), Aki Takahashi (University of Tsukuba), Teruhiro Okuyama (MIT), Charles Yokoyama (RIKEN BSI), Ai Koizumi (CiNet), and Tsai-Wen Chen (National Yang-Ming University) for comments, Tadashi Yamamoto (OIST) for sharing behavior testing setups, and Steven D. Aird (OIST) for editing the manuscript.

Competing interests: The authors declare no competing financial interests.

Funding: We acknowledge a JSPS KAKENHI Grant (JP 16J10077) by DC1 Student Research Fellowship to R.X.L. and OIST internal funding to B.K. The funders had no role in study design, data collection and interpretation, or the decision to submit the work for publication.

Author contributions: R.X.L. conceptualized the study, designed the research, performed experiments, analyzed data, interpreted results, wrote the original draft, and revised the article; G.J.S. advised on data analysis and revised the article; B.K. advised on research design and revised the article.

References:

1. DSM-III. Diagnostic and statistical manual of mental disorders (DSM-III). *Am. Psychiatr. Assoc.*
2. DSM-5. Diagnostic and statistical manual of mental disorders (DSM-5). *Am. Psychiatr. Assoc.* 947 (2013). doi:10.1176/appi.books.9780890425596
3. Schnyder, U. & Cloitre, M. *Evidence based treatments for trauma-related psychological disorders : a practical guide for clinicians*.

1026 4. Ehlers, A. & Clark, D. M. A cognitive model of posttraumatic stress disorder. *Behav.*
1027 *Res. Ther.* **38,** 319–345 (2000).
1028 5. Siegmund, A. & Wotjak, C. T. Toward an Animal Model of Posttraumatic Stress
1029 Disorder. *Ann. N. Y. Acad. Sci.* **1071,** 324–334 (2006).
1030 6. Hayes, J. P., VanElzakker, M. B. & Shin, L. M. Emotion and cognition interactions in
1031 PTSD: a review of neurocognitive and neuroimaging studies. *Front. Integr. Neurosci.* **6,**
1032 89 (2012).
1033 7. Zoladz, P. R. & Diamond, D. M. Current status on behavioral and biological markers of
1034 PTSD: A search for clarity in a conflicting literature. *Neurosci. Biobehav. Rev.* **37,** 860–
1035 895 (2013).
1036 8. Bryant, R. A., O'Donnell, M. L., Creamer, M., McFarlane, A. C. & Silove, D. A
1037 Multisite Analysis of the Fluctuating Course of Posttraumatic Stress Disorder. *JAMA*
1038 *Psychiatry* **70,** 839 (2013).
1039 9. Ben-Ami Bartal, I., Decety, J. & Mason, P. Empathy and pro-social behavior in rats.
1040 *Science* **334,** 1427–30 (2011).
1041 10. Ben-Ami Bartal, I., Rodgers, D. A., Bernardez Sarria, M. S., Decety, J. & Mason, P.
1042 Pro-social behavior in rats is modulated by social experience. *Elife* **3,** (2014).
1043 11. Burkett, J. P. *et al.* Oxytocin-dependent consolation behavior in rodents. *Science* **351,**
1044 375–8 (2016).
1045 12. Smith, M. L., Hostetler, C. M., Heinricher, M. M. & Ryabinin, A. E. Social transfer of
1046 pain in mice. *Sci. Adv.* **2,** e1600855–e1600855 (2016).
1047 13. Cryan, J. F. & Holmes, A. The ascent of mouse: advances in modelling human
1048 depression and anxiety. *Nat. Rev. Drug Discov.* **4,** 775–790 (2005).
1049 14. Kaouane, N. *et al.* Glucocorticoids can induce PTSD-like memory impairments in mice.
1050 *Science* **335,** 1510–3 (2012).

1051 15. Calhoon, G. G. & Tye, K. M. Resolving the neural circuits of anxiety. *Nat. Neurosci.*
1052 **18,** 1394–1404 (2015).
1053 16. Tovote, P., Fadok, J. P. & Lüthi, A. Neuronal circuits for fear and anxiety. *Nat. Rev.*
1054 *Neurosci.* **16,** 317–331 (2015).
1055 17. Davis, M. Sensitization of the acoustic startle reflex by footshock. *Behav. Neurosci.* **103,**
1056 495–503 (1989).
1057 18. Pamplona, F. A. *et al.* Prolonged fear incubation leads to generalized avoidance behavior
1058 in mice. *J. Psychiatr. Res.* **45,** 354–360 (2011).
1059 19. Warren, B. L. *et al.* Neurobiological Sequelae of Witnessing Stressful Events in Adult
1060 Mice. *Biol. Psychiatry* **73,** 7–14 (2013).
1061 20. Tsuda, M. C., Yeung, H.-M., Kuo, J. & Usdin, T. B. Incubation of Fear Is Regulated by
1062 TIP39 Peptide Signaling in the Medial Nucleus of the Amygdala. *J. Neurosci.* **35,**
1063 12152–61 (2015).
1064 21. Sillivan, S. E. *et al.* Susceptibility and Resilience to Posttraumatic Stress Disorder–like
1065 Behaviors in Inbred Mice. *Biol. Psychiatry* **82,** 924–933 (2017).
1066 22. Balogh, S. A., Radcliffe, R. A., Logue, S. F. & Wehner, J. M. Contextual and cued fear
1067 conditioning in C57BL/6J and DBA/2J mice: Context discrimination and the effects of
1068 retention interval. *Behav. Neurosci.* **116,** 947–957 (2002).
1069 23. Philbert, J. *et al.* Acute inescapable stress exposure induces long-term sleep disturbances
1070 and avoidance behavior: A mouse model of post-traumatic stress disorder (PTSD).
1071 *Behav. Brain Res.* **221,** 149–154 (2011).
1072 24. Sial, O. K., Warren, B. L., Alcantara, L. F., Parise, E. M. & Bolaños-Guzmán, C. A.
1073 Vicarious social defeat stress: Bridging the gap between physical and emotional stress.
1074 *J. Neurosci. Methods* **258,** 94–103 (2016).

1075 25. Houston, F. P., Stevenson, G. D., McNaughton, B. L. & Barnes, C. A. Effects of age on
1076 the generalization and incubation of memory in the F344 rat. *Learn. Mem.* **6,** 111–9
1077 (1999).
1078 26. Goto, T. *et al.* Subchronic and mild social defeat stress accelerates food intake and body
1079 weight gain with polydipsia-like features in mice. *Behav. Brain Res.* **270,** 339–348
1080 (2014).
1081 27. Otabi, H., Goto, T., Okayama, T., Kohari, D. & Toyoda, A. The acute social defeat stress
1082 and nest-building test paradigm: A potential new method to screen drugs for depressive-
1083 like symptoms. *Behav. Processes* **135,** 71–75 (2017).
1084 28. Ben-Ami Bartal, I. *et al.* Anxiolytic Treatment Impairs Helping Behavior in Rats. *Front.*
1085 *Psychol.* **7,** 850 (2016).
1086 29. DeMorrow, S., DeMorrow & Sharon. Role of the Hypothalamic–Pituitary–Adrenal Axis
1087 in Health and Disease. *Int. J. Mol. Sci.* **19,** 986 (2018).
1088 30. Ramos, A. Animal models of anxiety: do I need multiple tests? *Trends Pharmacol. Sci.*
1089 **29,** 493–8 (2008).
1090 31. Archer, J. Tests for emotionality in rats and mice: A review. *Anim. Behav.* **21,** 205–235
1091 (1973).
1092 32. Grupe, D. W. & Nitschke, J. B. Uncertainty and anticipation in anxiety: an integrated
1093 neurobiological and psychological perspective. *Nat. Rev. Neurosci.* **14,** 488–501 (2013).
1094 33. Kumar, V., Bhat, Z. A. & Kumar, D. Animal models of anxiety: A comprehensive
1095 review. *J. Pharmacol. Toxicol. Methods* **68,** 175–183 (2013).
1096 34. Pessoa, L. On the relationship between emotion and cognition. *Nat. Rev. Neurosci.* **9,**
1097 148–158 (2008).
1098 35. Cloninger, C. R. Anxiety and Theories of Emotion. *Handb. Anxiety* **2,** 1–29 (1988).

1099 36. Adler, L. A., Kunz, M., Chua, H. C., Rotrosen, J. & Resnick, S. G. Attention-
1100 Deficit/Hyperactivity Disorder in adult patients with Posttraumatic stress disorder
1101 (PTSD): Is ADHD a vulnerability factor? *J. Atten. Disord.* **8,** 11–16 (2004).
1102 37. Mostoufi, S. *et al.* Pain sensitivity in posttraumatic stress disorder and other anxiety
1103 disorders: a preliminary case control study. *Ann. Gen. Psychiatry* **13,** 31 (2014).
1104 38. Andrews, B., Brewin, C. R., Philpott, R. & Stewart, L. Delayed-Onset Posttraumatic
1105 Stress Disorder: A Systematic Review of the Evidence. *Am. J. Psychiatry* **164,** 1319–
1106 1326 (2007).
1107 39. Bryant, R. A. *et al.* Acute and Chronic Posttraumatic Stress Symptoms in the Emergence
1108 of Posttraumatic Stress Disorder. *JAMA Psychiatry* **74,** 135 (2017).
1109 40. Anderson, D. J. Circuit modules linking internal states and social behaviour in flies and
1110 mice. *Nat. Rev. Neurosci.* **17,** 692–704 (2016).
1111 41. Krishnan, V. *et al.* Molecular adaptations underlying susceptibility and resistance to
1112 social defeat in brain reward regions. *Cell* **131,** 391–404 (2007).
1113 42. Sandi, C. & Haller, J. Stress and the social brain: behavioural effects and neurobiological
1114 mechanisms. *Nat. Rev. Neurosci.* **16,** 290–304 (2015).
1115 43. Yang, T. *et al.* Social Control of Hypothalamus-Mediated Male Aggression. *Neuron* **95,**
1116 955–970.e4 (2017).
1117 44. Chung, M. C. *et al.* Coping with post-traumatic stress symptoms following relationship
1118 dissolution. *Stress Heal.* **19,** 27–36 (2003).
1119 45. Kogan, J. H., Franklandand, P. W. & Silva, A. J. Long-term memory underlying
1120 hippocampus-dependent social recognition in mice. *Hippocampus* **10,** 47–56 (2000).
1121 46. Okuyama, T., Kitamura, T., Roy, D. S., Itohara, S. & Tonegawa, S. Ventral CA1 neurons
1122 store social memory. *Science* **353,** 1536–1541 (2016).
1123 47. Cohen, S. & Wills, T. A. *Stress, Social Support, and the Buffering Hypothesis*.
1124 *Psychologkal Bulletin* **98,** (1985).

1125 48. Yu, Y.-Q., Barry, D. M., Hao, Y., Liu, X.-T. & Chen, Z.-F. Molecular and neural basis
1126 of contagious itch behavior in mice. *Science* **355,** 1072–1076 (2017).
1127 49. Li, Y. *et al.* Serotonin neurons in the dorsal raphe nucleus encode reward signals. *Nat.*
1128 *Commun.* **7,** 10503 (2016).
1129 50. Fischer, A. G. & Ullsperger, M. An Update on the Role of Serotonin and its Interplay
1130 with Dopamine for Reward. *Front. Hum. Neurosci.* **11,** 484 (2017).
1131 51. McIntyre, D. C. & Kelly, M. E. The Parahippocampal Cortices and Kindling. *Ann. N. Y.*
1132 *Acad. Sci.* **911,** 343–354 (2006).
1133 52. McIntyre, D. C. The Kindling Phenomenon. *Model. Seizures Epilepsy* 351–363 (2006).
1134 doi:10.1016/B978-012088554-1/50030-X
1135 53. Rau, V., DeCola, J. P. & Fanselow, M. S. Stress-induced enhancement of fear learning:
1136 An animal model of posttraumatic stress disorder. *Neurosci. Biobehav. Rev.* **29,** 1207–
1137 1223 (2005).
1138 54. Knox, D. *et al.* Single prolonged stress disrupts retention of extinguished fear in rats.
1139 *Learn. Mem.* **19,** 43–9 (2012).
1140 55. Walf, A. A. & Frye, C. A. The use of the elevated plus maze as an assay of anxiety-
1141 related behavior in rodents. *Nat. Protoc.* **2,** 322–328 (2007).
1142 56. Garcia, A. M. B., Martinez, R. C. R. & Morato, S. Preference for the light compartment
1143 of a light/dark cage does not affect rat exploratory behavior in the elevated plus-maze.
1144 *Psychol. & Neurosci.* **1,** 73–80 (2008).
1145 57. Hascoët, M., Bourin, M. & Nic Dhonnchadha, B. Á. The mouse ligth-dark paradigm: A
1146 review. *Prog. Neuro-Psychopharmacology Biol. Psychiatry* **25,** 141–166 (2001).
1147 58. Crusio, W. E. in *Behavioral Genetics of the Mouse* (eds. Crusio, W. E., Sluyter, F.,
1148 Gerlai, R. T. & Pietropaolo, S.) 148–154 (Cambridge University Press, 2013).
1149 doi:10.1017/CBO9781139541022.016

1150 59. Kulesskaya, N. & Voikar, V. Assessment of mouse anxiety-like behavior in the light–
1151 dark box and open-field arena: Role of equipment and procedure. *Physiol. Behav.* **133,**
1152 30–38 (2014).
1153 60. Ennaceur, A. Tests of unconditioned anxiety — Pitfalls and disappointments. *Physiol.*
1154 *Behav.* **135,** 55–71 (2014).
1155 61. Carobrez, A. P. & Bertoglio, L. J. Ethological and temporal analyses of anxiety-like
1156 behavior: The elevated plus-maze model 20 years on. *Neurosci. Biobehav. Rev.* **29,**
1157 1193–1205 (2005).
1158 62. Engin, E. & Treit, D. The effects of intra-cerebral drug infusions on animals'
1159 unconditioned fear reactions: A systematic review. *Prog. Neuro-Psychopharmacology*
1160 *Biol. Psychiatry* **32,** 1399–1419 (2008).
1161 63. Henriques-Alves, A. M. & Queiroz, C. M. Ethological Evaluation of the Effects of
1162 Social Defeat Stress in Mice: Beyond the Social Interaction Ratio. *Front. Behav.*
1163 *Neurosci.* **9,** 364 (2016).
1164 64. Hånell, A. & Marklund, N. Structured evaluation of rodent behavioral tests used in drug
1165 discovery research. *Front. Behav. Neurosci.* **8,** 252 (2014).
1166 65. Anderson, D. J. & Perona, P. Toward a Science of Computational Ethology. *Neuron* **84,**
1167 18–31 (2014).
1168 66. Golden, S. A., Covington, H. E., Berton, O. & Russo, S. J. A standardized protocol for
1169 repeated social defeat stress in mice. *Nat. Protoc.* **6,** 1183–1191 (2011).
1170 67. Anderson, D. J. & Adolphs, R. A framework for studying emotions across species. *Cell*
1171 **157,** 187–200 (2014).
1172 68. Mataix-Cols, D. *et al.* D-Cycloserine Augmentation of Exposure-Based Cognitive
1173 Behavior Therapy for Anxiety, Obsessive-Compulsive, and Posttraumatic Stress
1174 Disorders. *JAMA Psychiatry* **74,** 501 (2017).

1175 69. Hetrick, S. E., Purcell, R., Garner, B. & Parslow, R. Combined pharmacotherapy and
1176 psychological therapies for post traumatic stress disorder (PTSD). *Cochrane Database*
1177 *Syst. Rev.* (2010). doi:10.1002/14651858.CD007316.pub2
1178 70. Funamizu, A., Kuhn, B. & Doya, K. Neural substrate of dynamic Bayesian inference in
1179 the cerebral cortex. *Nat. Neurosci.* **19,** 1682–1689 (2016).
1180 71. Larkum, M. A cellular mechanism for cortical associations: an organizing principle for
1181 the cerebral cortex. *Trends Neurosci.* **36,** 141–151 (2013).
1182 72. Lee, R. X., Huang, J.-J., Huang, C., Tsai, M.-L. & Yen, C.-T. Plasticity of cerebellar
1183 Purkinje cells in behavioral training of body balance control. *Front. Syst. Neurosci.* **9,**
1184 1–15 (2015).
1185 73. Lee, R. X., Huang, J. J., Huang, C., Tsai, M. L. & Yen, C. T. Collateral projections from
1186 vestibular nuclear and inferior olivary neurons to lobules I/II and IX/X of the rat
1187 cerebellar vermis: A double retrograde labeling study. *Eur. J. Neurosci.* **40,** 2811–2821
1188 (2014).
1189 74. Donaldson, G. P., Melanie Lee, S. & Mazmanian, S. K. Gut biogeography of the
1190 bacterial microbiota. *Nat. Publ. Gr.* **14,** (2015).
1191 75. Tononi, G., Boly, M., Massimini, M. & Koch, C. Integrated information theory: from
1192 consciousness to its physical substrate. *Nat. Rev. Neurosci.* **17,** 450–461 (2016).
1193 76. Murugan, M. *et al.* Combined Social and Spatial Coding in a Descending Projection
1194 from the Prefrontal Cortex. *Cell* **171,** 1663–1677.e16 (2017).
1195 77. Zelikowsky, M. *et al.* The Neuropeptide Tac2 Controls a Distributed Brain State Induced
1196 by Chronic Social Isolation Stress. *Cell* **173,** 1265–1279.e19 (2018).
1197 78. Kohl, J. *et al.* Functional circuit architecture underlying parental behaviour. *Nature* **556,**
1198 326–331 (2018).
1199 79. Remedios, R. *et al.* Social behaviour shapes hypothalamic neural ensemble
1200 representations of conspecific sex. *Nature* **550,** 388–392 (2017).

1201 80. Matias, S., Lottem, E., Dugué, G. P. & Mainen, Z. F. Activity patterns of serotonin
1202 neurons underlying cognitive flexibility. *Elife* **6,** e20552 (2017).
1203 81. Roome, C. J. & Kuhn, B. Simultaneous dendritic voltage and calcium imaging and
1204 somatic recording from Purkinje neurons in awake mice. *Nat. Commun.* **9,** 3388 (2018).
1205 82. Shin, L. M., Rauch, S. L. & Pitman, R. K. Amygdala, Medial Prefrontal Cortex, and
1206 Hippocampal Function in PTSD. *Ann. N. Y. Acad. Sci.* **1071,** 67–79 (2006).
1207 83. Gilbertson, M. W. *et al.* Smaller hippocampal volume predicts pathologic vulnerability
1208 to psychological trauma. *Nat. Neurosci.* **5,** 1242–1247 (2002).
1209 84. Pavić, L. *et al.* Smaller right hippocampus in war veterans with posttraumatic stress
1210 disorder. *Psychiatry Res. Neuroimaging* **154,** 191–198 (2007).
1211 85. McFarlane, A. C. The long-term costs of traumatic stress: intertwined physical and
1212 psychological consequences. *World Psychiatry* **9,** 3–10 (2010).
1213 86. Takahashi, A. *et al.* Glutamate input in the dorsal raphe nucleus as a determinant of
1214 escalated aggression in male mice. *J. Neurosci.* **35,** 6452–63 (2015).
1215 87. Miczek, K. A. & O'Donnell, J. M. Intruder-evoked aggression in isolated and
1216 nonisolated mice: Effects of psychomotor stimulants and l-Dopa. *Psychopharmacology*
1217 *(Berl).* **57,** 47–55 (1978).
1218 88. Crawley, J. & Goodwin, F. K. Preliminary report of a simple animal behavior model for
1219 the anxiolytic effects of benzodiazepines. *Pharmacol. Biochem. Behav.* **13,** 167–170
1220 (1980).
1221 89. Pellow, S., Chopin, P., File, S. E. & Briley, M. Validation of open : closed arm entries
1222 in an elevated plus-maze as a measure of anxiety in the rat. *J. Neurosci. Methods* **14,**
1223 149–167 (1985).
1224 90. Hall, C. & Ballachey, E. L. A study of the rat's behavior in a field. A contribution to
1225 method in comparative psychology. *Univ. Calif. Publ. Psychol.* 1–12 (1932).

1226 91. Arakawa, T. *et al.* A male-specific QTL for social interaction behavior in mice mapped
1227 with automated pattern detection by a hidden Markov model incorporated into newly
1228 developed freeware. *J. Neurosci. Methods* **234,** 127–134 (2014).
1229 92. Tsuda, M. C. & Ogawa, S. Long-Lasting Consequences of Neonatal Maternal
1230 Separation on Social Behaviors in Ovariectomized Female Mice. *PLoS One* **7,** e33028
1231 (2012).
1232 93. Berton, O. *et al.* Essential role of BDNF in the mesolimbic dopamine pathway in social
1233 defeat stress. *Science* **311,** 864–8 (2006).
1234 94. Nadler, J. J. *et al.* Automated apparatus for quantitation of social approach behaviors in
1235 mice. *Genes, Brain Behav.* **3,** 303–314 (2004).
1236 95. Basser, P. J., Mattiello, J. & LeBihan, D. MR diffusion tensor spectroscopy and imaging.
1237 *Biophys. J.* **66,** 259–267 (1994).
1238 96. Hrabe, J., Kaur, G. & Guilfoyle, D. N. Principles and limitations of NMR diffusion
1239 measurements. *J. Med. Phys.* **32,** 34–42 (2007).
1240 97. Mori, S. (Susumu). *Introduction to diffusion tensor imaging*. (Elsevier, 2007).

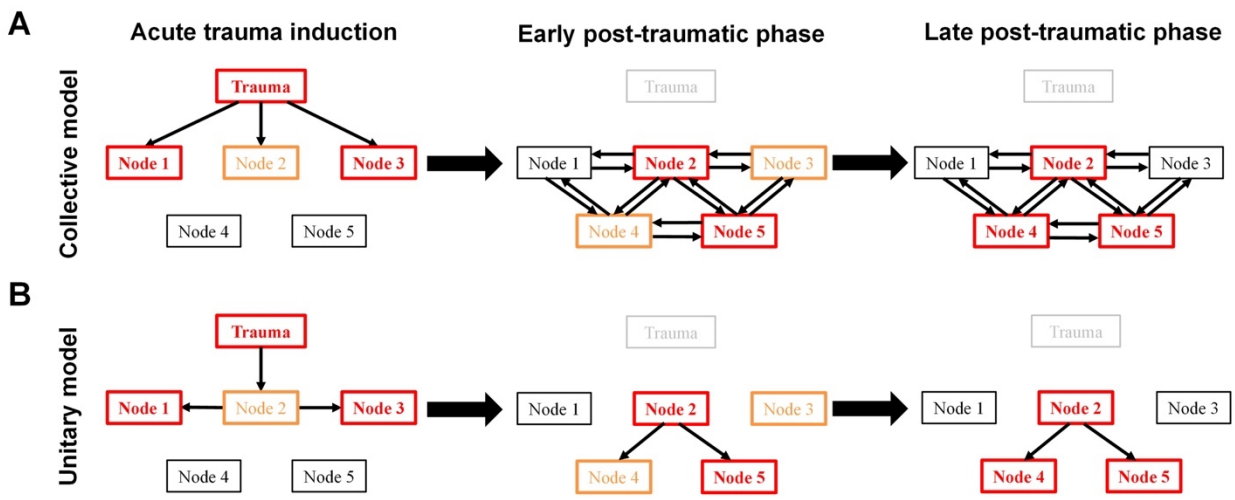

Figure 1. **Two conceptual models of the post-traumatic stress incubation process. (A)** In the collective model, different psychological elements (Node #, a type of emotion or cognition) influence each other during different phases of stress incubation. **(B)** In the unitary model a single common factor underlies the development of post-traumatic behaviors. Orange and red boxes represent medium and strong trauma-induced differences, respectively. It is assumed that each psychological element can be connected to an associated neural substrate with trauma-induced dynamic changes.

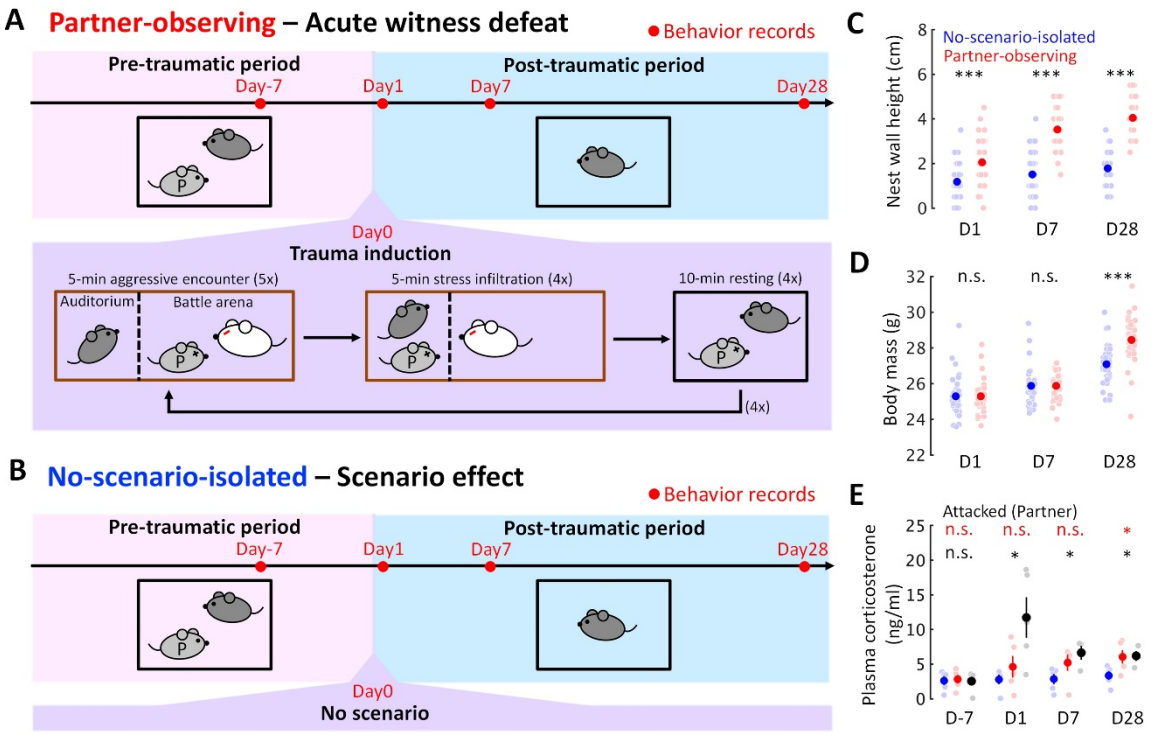

Figure 2. Paradigm induces long-term and delayed effects on multiple behaviors and physical conditions. (A) Paradigm with acute psychosocial trauma induction in mice. Focal mouse (dark gray; the Partner-observing mouse), partner mouse (light gray P), aggressor mouse (white), focal mouse's homecage (black), aggressor's homecage (brown), and wire-meshed divider (dashed line). **(B)** Experiments of No-scenario-isolated mice which had no experience of trauma induction identified the scenario effect in the behavioral paradigm. **(C)** Nest wall heights show long-lasting significant differences after trauma induction. **(D)** Body mass shows a significant increase 28 days after trauma induction. **(E)** Baseline plasma corticosterone level increased after trauma induction for both Partner-observing mice and their partners, the Attacked mice. Error bars indicate standard errors of the means; n.s., $p \geq 0.05$; *, $0.01 \leq p < 0.05$; ***, $p < 0.001$; two-tailed, two-sample Student's t-test.

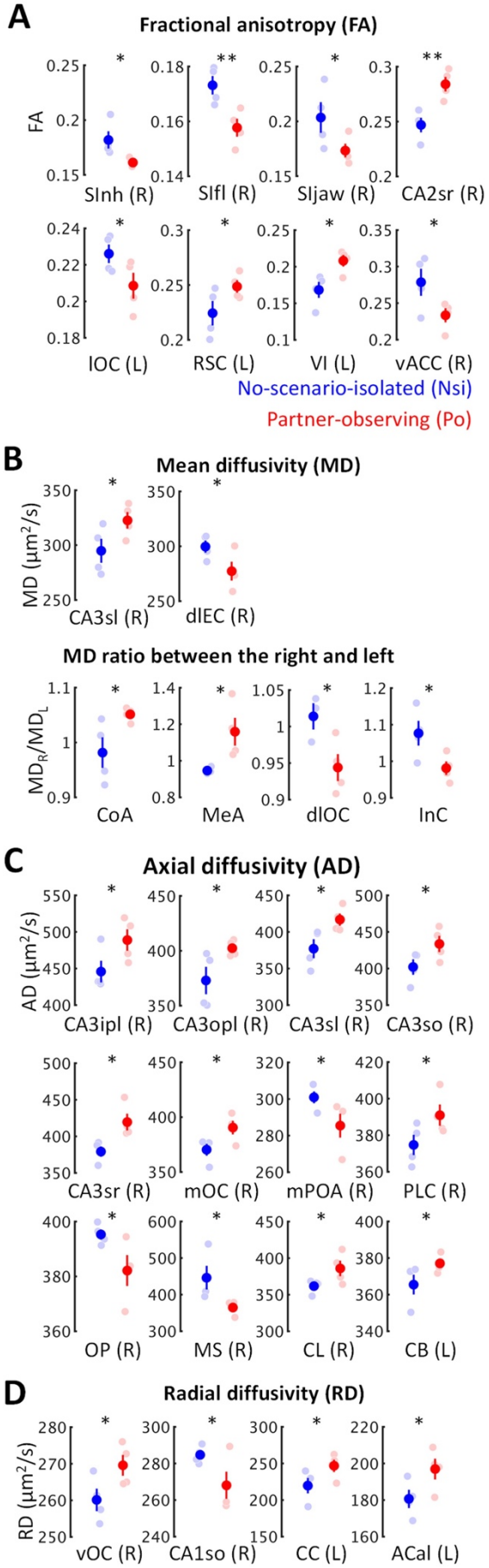
A
Fractional anisotropy (FA)
FA
SInh (R)
SIfl (R)
SIjaw (R)
CA2sr (R)
IOC (L)
RSC (L)
VI (L)
vACC (R)
No-scenario-isolated (Nsi)
Partner-observing (Po)
B
Mean diffusivity (MD)
MD (μm²/s)
CA3sl (R)
dlEC (R)
MD ratio between the right and left
MD_R/MD_L
CoA
MeA
dlOC
InC
C
Axial diffusivity (AD)
AD (μm²/s)
CA3ipl (R)
CA3opl (R)
CA3sl (R)
CA3so (R)
CA3sr (R)
mOC (R)
mPOA (R)
PLC (R)
OP (R)
MS (R)
CL (R)
CB (L)
D
Radial diffusivity (RD)
RD (μm²/s)
vOC (R)
CA1so (R)
CC (L)
ACal (L)

1261

1262 **Figure 3. Diffusion tensor imaging (DTI) reveals chronic effect of acute observational**
1263 **stress on microstructures in the brain.** Graphs show all brain structures with significant
1264 differences between No-scenario-isolated mice (n=4) and Partner-observing mice (n=4). **(A)**
1265 Fractional anisotropy (FA) of DTI-based water diffusivity suggests the changes of average
1266 microstructural integrity in multiple areas of the cerebral cortex. lOC, lateral orbital cortex;
1267 SInh, non-homunculus region of the primary sensory cortex; SIfl, forelimb region of the
1268 primary sensory cortex; SIjaw, jaw region of the primary sensory cortex; vACC, ventral region
1269 of the anterior cingulate cortex; CA2sr, stratum radiatum of the hippocampal cornu ammonis
1270 (CA) 2 area; RSC, the retrosplenial cortex; VI, the primary visual cortex; (R), the right area;
1271 (L), the left area. **(B)** DTI-based mean water diffusivity (MD) suggests the changes of
1272 membrane density in multiple areas of the entorhinal cortex-hippocampus system and the
1273 straitening of structural hemispheric specializations in the amygdala-insular cortex system.
1274 dlOC, dorsolateral orbital cortex; InC, the insular cortex; CoA, the cortical amygdalar nucleus;
1275 MeA, medial amygdalar nucleus; CA3sl, stratum lucidum of the hippocampal CA3 area; dlEC,
1276 dorsolateral entorhinal cortex. **(C)** DTI-based axial water diffusivity (AD) suggests the
1277 changes of neurite organization in multiple areas of the cerebral cortex and white matter mainly
1278 in the right hemisphere. OP, olfactory peduncle; PLC, prelimbic cortex; mOC, medial orbital
1279 cortex; CL, claustrum; MS, medial septal complex; mPOA, medial preoptic area; CB, cingulum
1280 bundle; CA3sr, stratum radiatum of the hippocampal CA3 area; CA3sl, stratum lucidum of the
1281 hippocampal CA3 area;CA3so, stratum oriens of the hippocampal CA3 area; CA3ipl, inner
1282 pyramidal layer of the hippocampal CA3 area; CA3opl, outer pyramidal layer of the
1283 hippocampal CA3 area. **(D)** DTI-based radial water diffusivity (RD) suggests the changes of
1284 myelination in multiple areas of the cerebral cortex in the right hemisphere and the white matter
1285 in the left hemisphere. vOC, ventral orbital cortex; ACal, anterior limb of the anterior
1286 commissure; CC, corpus callosum; CA1so, stratum oriens of the hippocampal CA1 area. *,
1287 $0.01 \leq p < 0.05$; **, $0.001 \leq p < 0.01$.

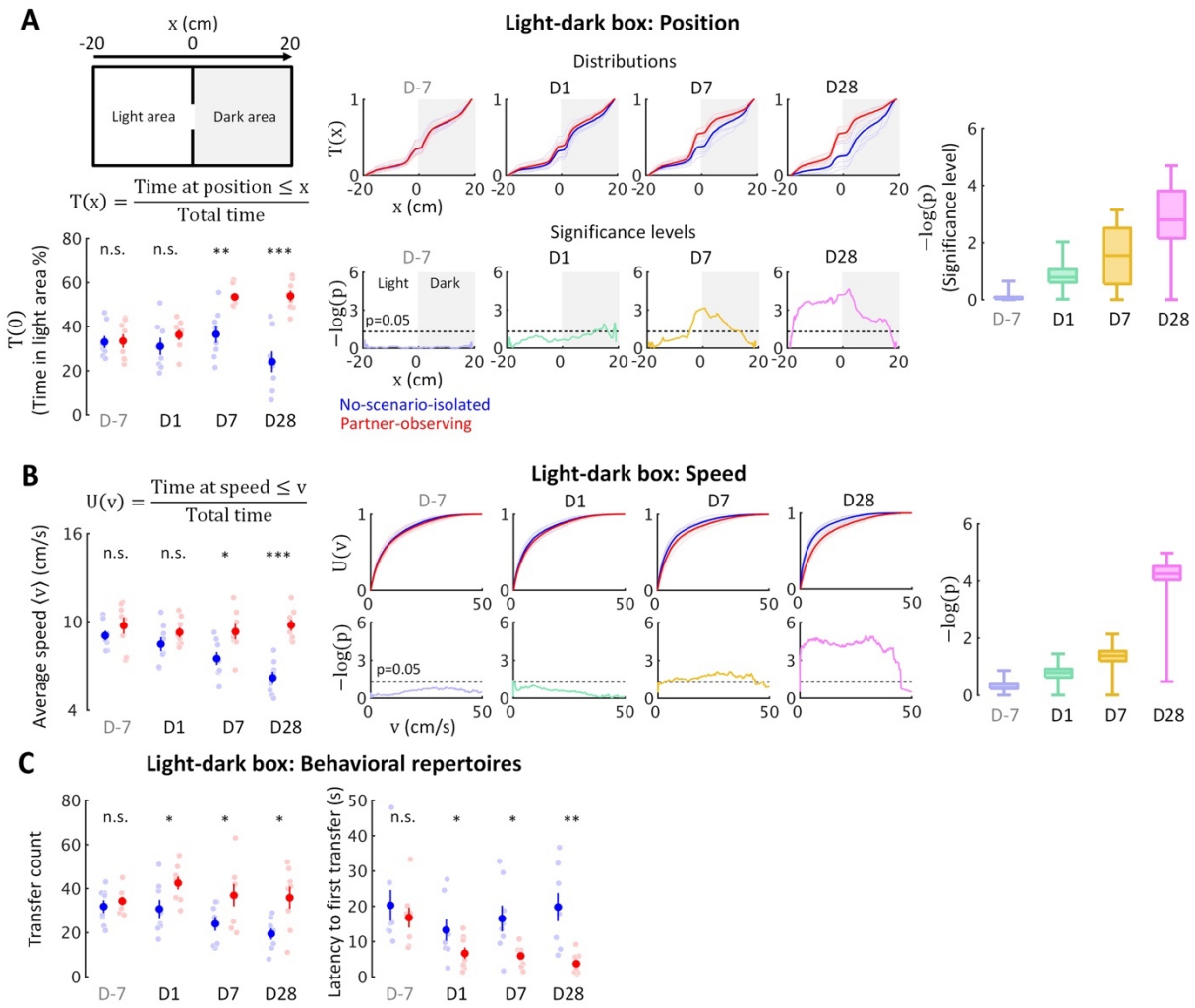

Figure 4. Fine-scale behavioral analysis in light-dark box test detects the gradually developing process of the behavioral difference. (A) Light-dark box test quantified through the cumulative position probability T(x) along the light-dark axis (left; total time = 300 s). On average, Partner-observing mice (red) spent more time in the light area than No-scenario-isolated mice (blue) during the late post-traumatic period [T(0), bottom-left]. Spatially fine-scale behavioral analysis reveals significant differences between Partner-observing and No-scenario-isolated populations already in the early post-traumatic period (middle). For each position, we compute the mean T(x) across the No-scenario-isolated and Partner-observing populations and compute statistical significance through a two-population Student's t-test. These differences gradually increased, as evidenced by significance distributions collapsed across all positions (right; box plots show the minima, lower quartiles, medians, upper quartiles,

1300 and maxima). **(B)** We similarly quantified speed using the fine-scale cumulative distribution
1301 U(v)of having speed ≤v and we show the statistical analysis of population differences in U(v).
1302 Cumulative distribution functions of locomotion speed (U(v) of having speed ≤v) and
1303 corresponding significance distributions provide an additional independent behavioral index
1304 that showed a gradually increasing differences of higher speed in Partner-observing mice. **(C)**
1305 Higher transfer counts and shorter latency to the first transfers in Partner-observing mice
1306 suggest their higher activity and exploratory motivation, respectively.

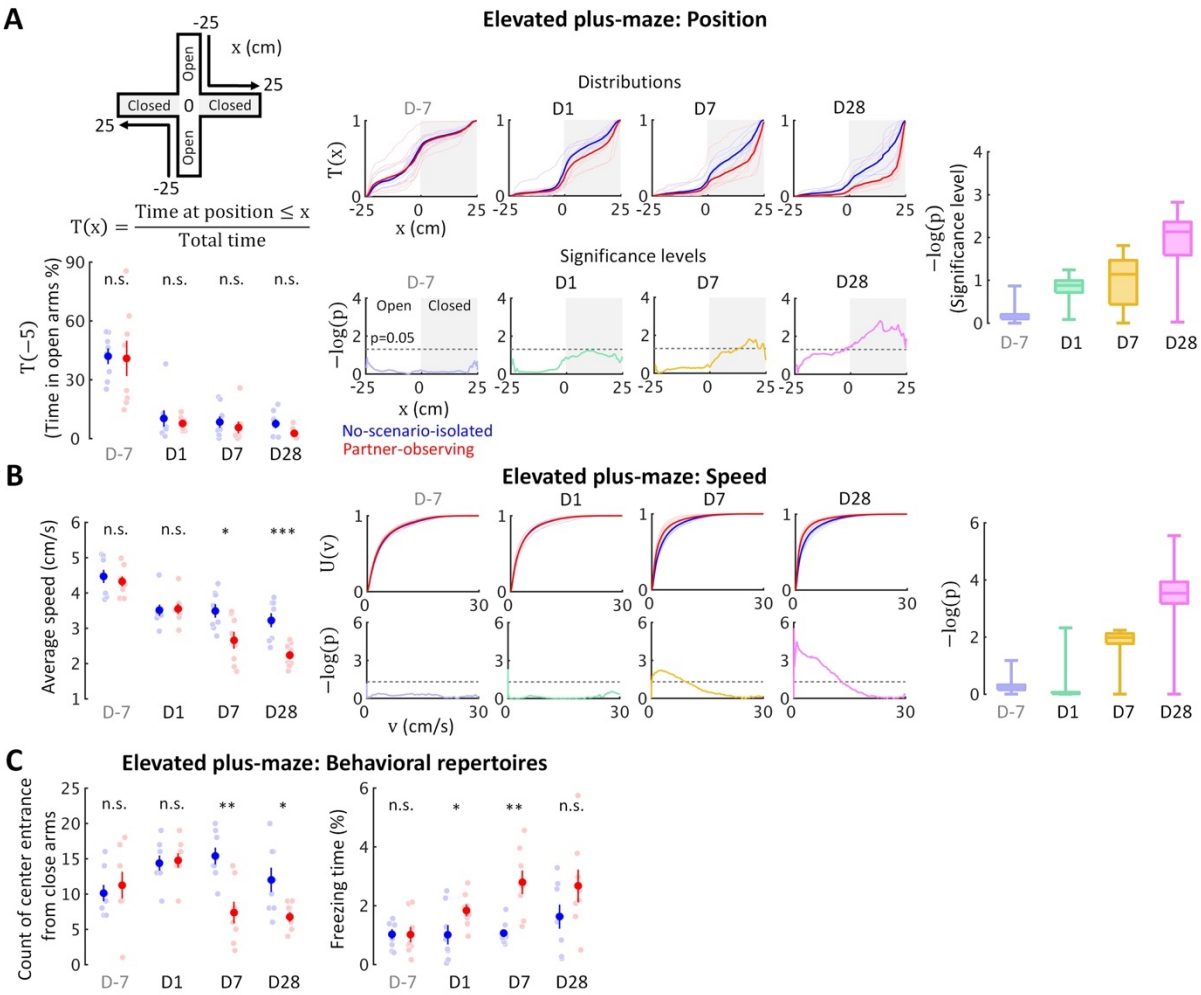

Figure 5. Behavioral testing in the elevated plus-maze demonstrates that stress incubation of anxiety caused the observed differences. (A) Partner-observing and No-scenario-isolated mice did not differ significantly in the time they spent in opened arms (total time = 300 s); however, spatial distributions show differences in preferred location between Partner-observing and No-scenario-isolated mice in the closed arms, which increased with time. **(B)** Cumulative distribution functions of locomotion speed and corresponding significance distributions show a gradually increasing differences of lower speeds in Partner-observing mice. **(C)** Less exploration from close arms to platform center and longer freezing time in Partner-observing mice suggest their stronger stress reactions.

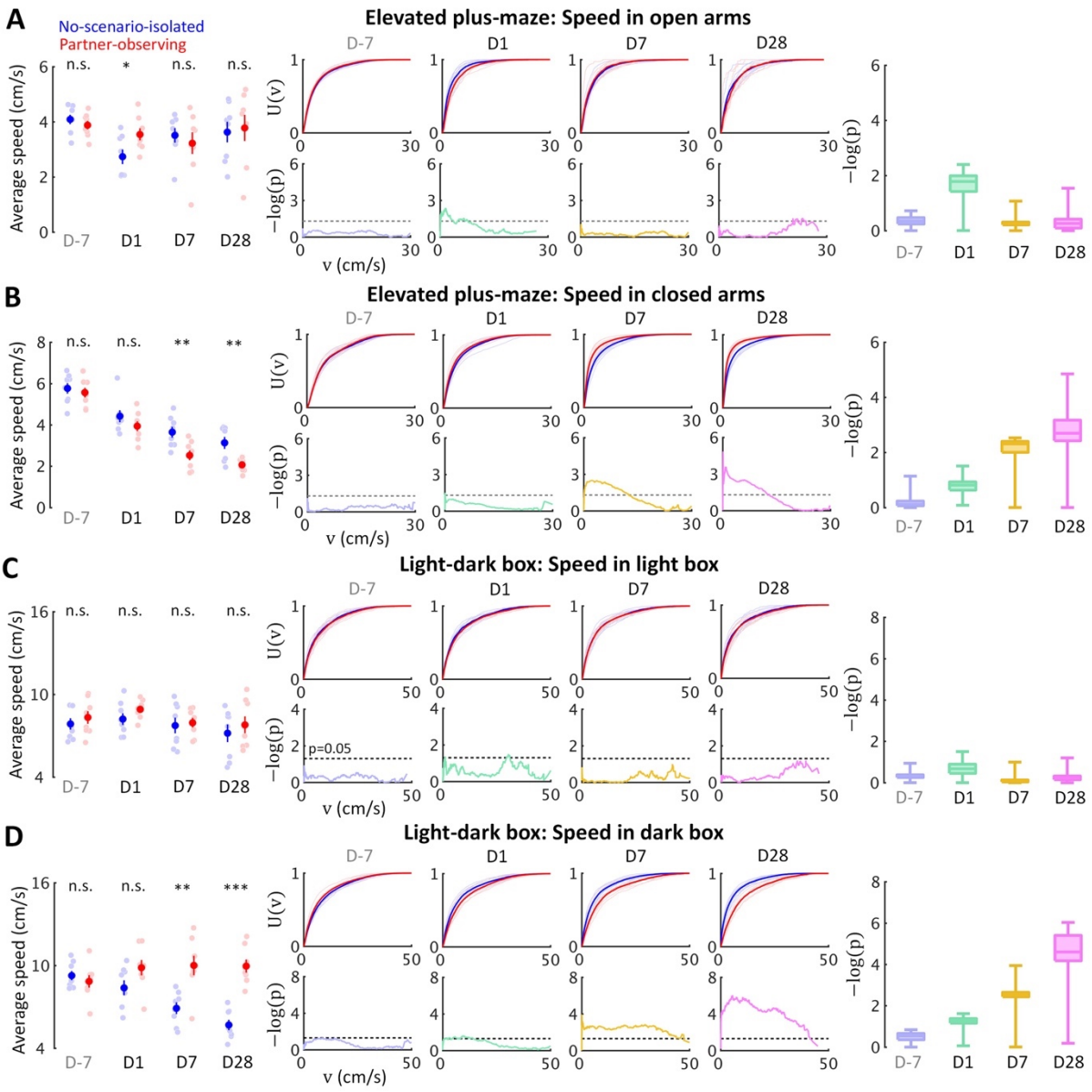

Figure 6. Gradually increasing anxiety and acute fear reaction were untangled in standard behavioral tests as different psychological components with distinctive developments. Locomotion speed shows acute difference only in stressor zones [open arms **(A)** and light area **(C)**], but incubated differences in stressor-free zones [dark area **(B)** and closed arms **(D)**].

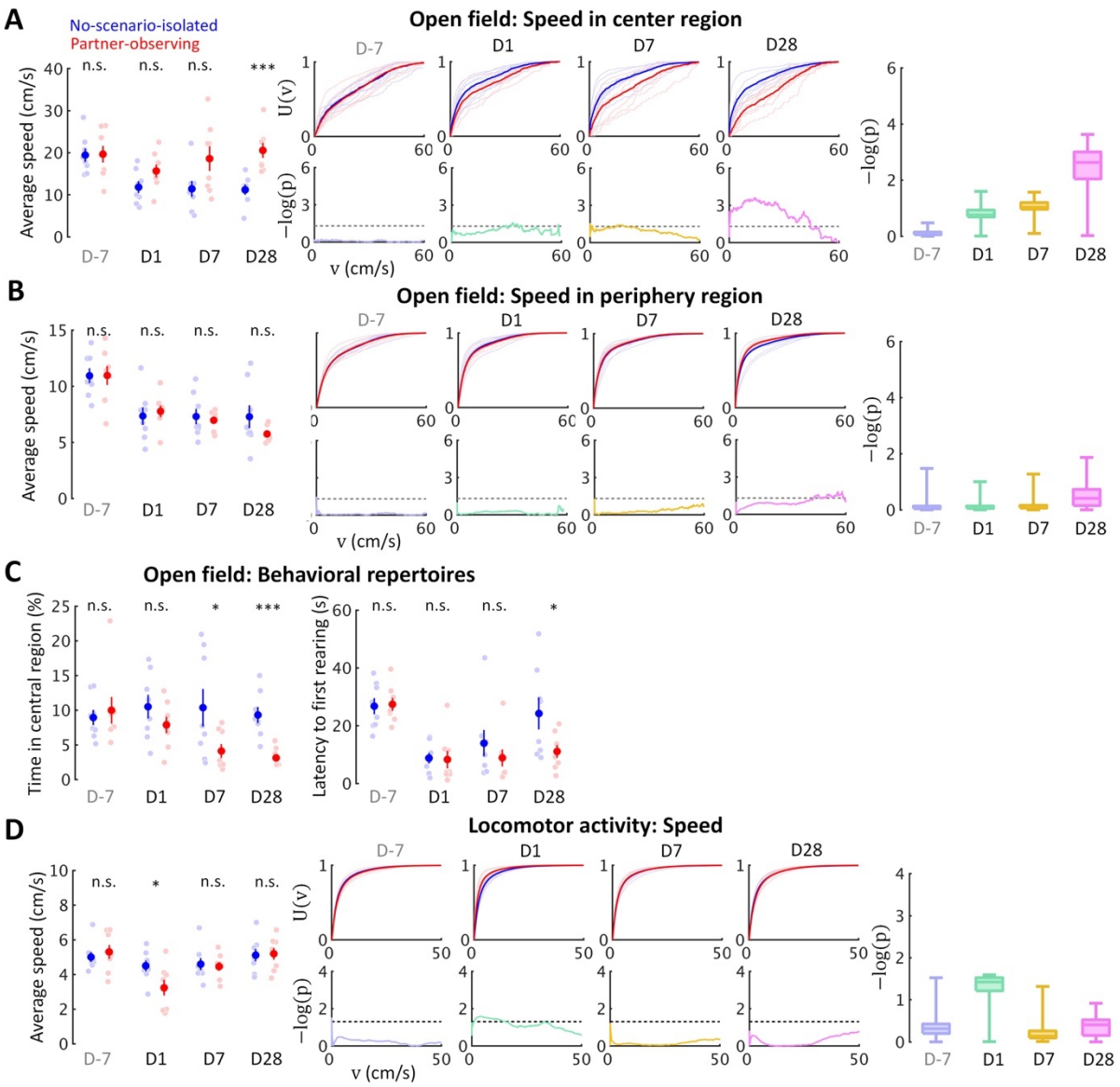

Figure 7. Behavioral testing in the open field test and locomotor activity test confirms distinctive psychological substrates and their corresponding development patterns. (A) Anxiety is evident in the open field test through a delayed onset of locomotor speed differences in the center region with higher spatial uncertainty. **(B)** The differences of locomotor speed observed in the center region did not occur in the periphery region with lower spatial uncertainty. **(C)** Less time spent in the central region by Partner-observing mice suggests their avoidance of a region with high special uncertainty, while shorter latency to their first rearing indicates their higher exploratory motivation. **(D)** In the locomotor activity test without stressors, acute effects of activity reduction recovered in the later post-traumatic period.

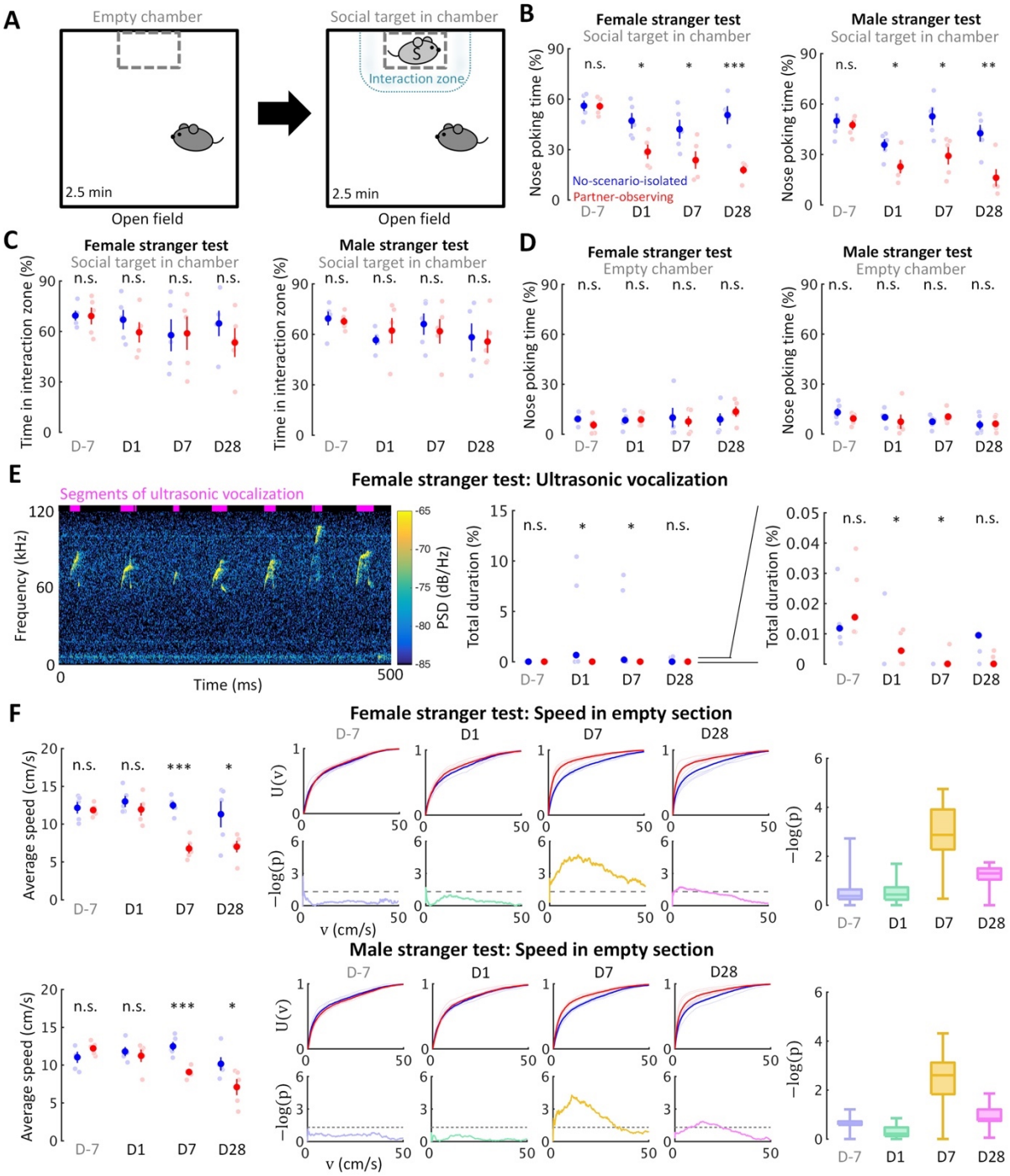

Figure 8. Acute psychosocial trauma decreases social interest. (A) The active social interaction test with consecutive non-social and social phases. During the social phase, motivation for social contact toward a stranger mouse (light gray S) was evaluated as the time spent for social approaches of nose poking and the time spent in the delineated interaction zone. **(B)** Partner-observing mice made fewer nose poking to both female (left) and male (right)

strangers. **(C)** There was no significant difference in the time spent in the interaction zone during the social phase, suggesting a decrease of social interest instead of an active social avoidance. **(D)** There was no significant difference in the time spent of nose poking during the non-social phase, confirming that the observed differences of nose poking time stemmed from a specifically social root. **(E)** Spectrogram of short but conspicuous ultrasonic vocalizations emphasizes a specific behavioral repertoire during the social session in the female stranger test of a No-scenario-isolated mouse on Day1. More vocalization was recorded from No-scenario-isolated mice than Partner-observing mice on Days 1 and 7. Reduced ultrasonic vocalization during the social session of the female stranger test in Partner-observing mice attests to diminished social communication. Note that data points greater than 0.05% are not visible in the right panel which zoom in the data of the middle panel to emphasize the data distributions in the range of 0–0.05%. Data points and median, one-tailed Mann-Whitney U test; PSD, power spectral density. **(F)** Partner-observing mice showed a delayed onset of reduction in locomotion speed during the non-social phase.

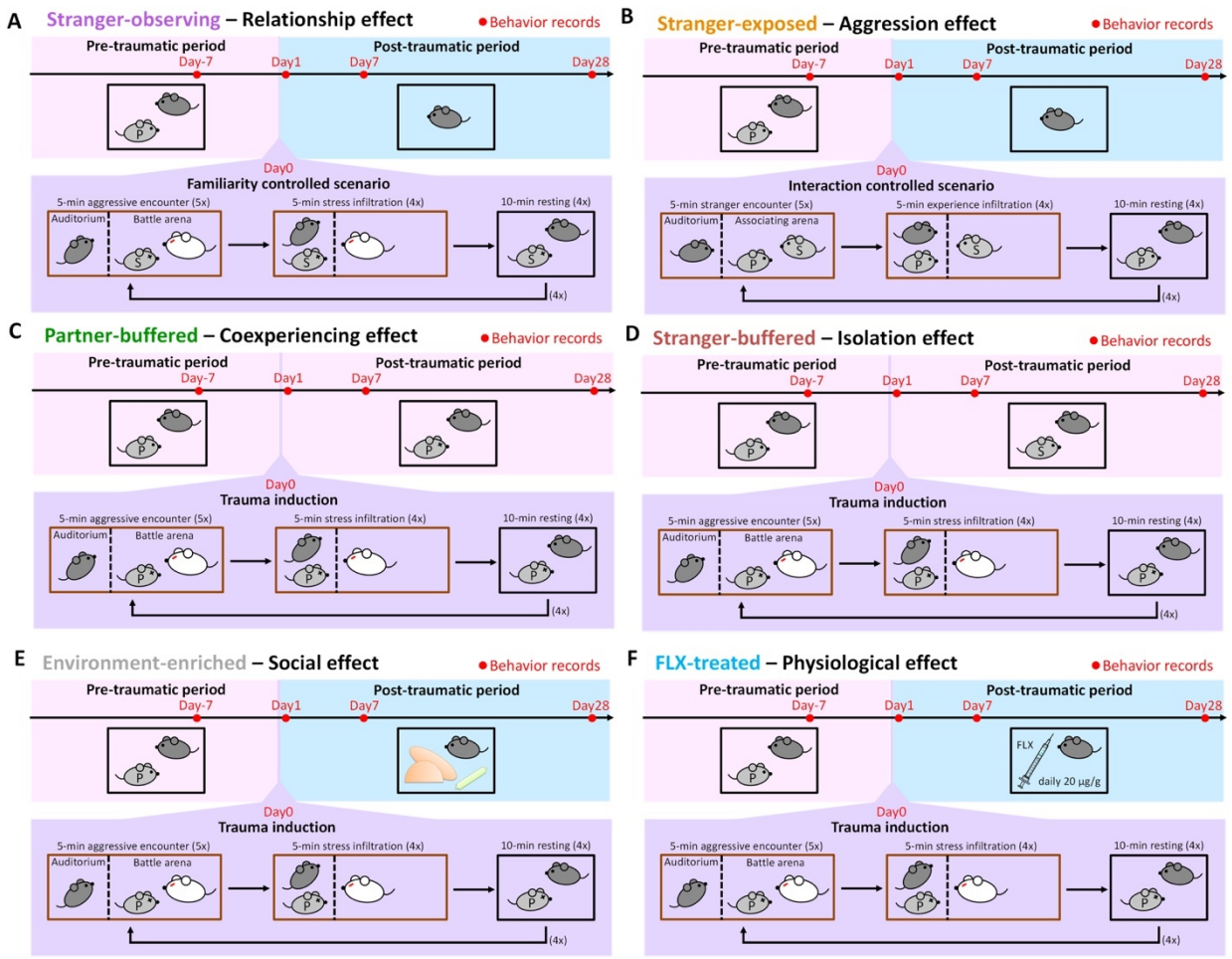

Figure 9. Control experiments investigate psychosocial and physiological factors that determined and recued the behavioral developments. (A) Experiments of Stranger-observing mice which had witnessing experience of trauma that happened to strangers, rather than to their pair-housed partners, identified the relationship effect in the behavioral paradigm. **(B)** Experiments of Stranger-exposed mice which had experience of social interactions without witnessing stress from strangers identified the aggression effect in the behavioral paradigm. **(C)** Experiments of Partner-buffered mice which were pair-housed with their partners after trauma induction identified the social transfer effect of coexperiencing trauma in the behavioral paradigm. **(D)** Experiments of Stranger-buffered mice which were pair-housed with strangers after trauma induction identified the isolation effect in the behavioral paradigm. **(E)** Experiments of Environment-enriched mice which were provided with toys after trauma induction identified the social rescue effect in the behavioral paradigm. **(F)** Experiments of

1366 FLX-treated mice which were treated with fluoxetine after trauma induction identified the
1367 pharmacological rescue effect in the behavioral paradigm.

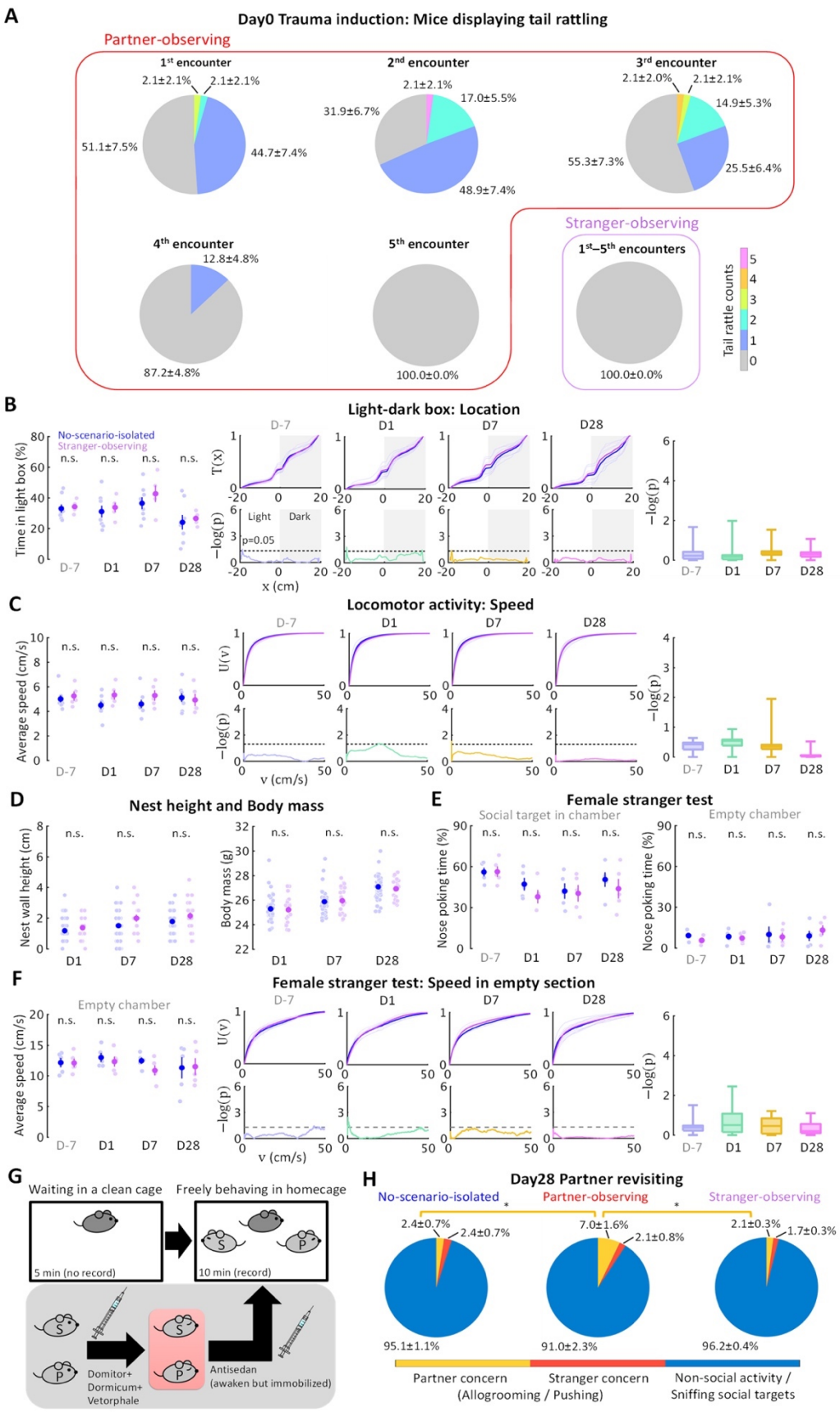
A
Day0 Trauma induction: Mice displaying tail rattling
Partner-observing
1st encounter
2.1±2.1%
2.1±2.1%
51.1±7.5%
44.7±7.4%
2nd encounter
2.1±2.1%
17.0±5.5%
31.9±6.7%
48.9±7.4%
3rd encounter
2.1±2.0%
2.1±2.1%
14.9±5.3%
55.3±7.3%
25.5±6.4%
4th encounter
12.8±4.8%
87.2±4.8%
5th encounter
100.0±0.0%
Stranger-observing
1st–5th encounters
100.0±0.0%
Tail rattle counts
5
4
3
2
1
0
B
Light-dark box: Location
No-scenario-isolated
Stranger-observing
Time in light box (%)
n.s.
D-7
D1
D7
D28
T(x)
Light
Dark
p=0.05
x (cm)
−log(p)
C
Locomotor activity: Speed
Average speed (cm/s)
U(v)
v (cm/s)
D
Nest height and Body mass
Nest wall height (cm)
Body mass (g)
E
Female stranger test
Social target in chamber
Empty chamber
Nose poking time (%)
F
Female stranger test: Speed in empty section
Empty chamber
Average speed (cm/s)
G
Waiting in a clean cage
Freely behaving in homecage
5 min (no record)
10 min (record)
S
P
Domitor+
Dormicum+
Vetorphale
Antisedan
(awaken but immobilized)
H
Day28 Partner revisiting
No-scenario-isolated
Partner-observing
Stranger-observing
2.4±0.7%
2.4±0.7%
95.1±1.1%
7.0±1.6%
2.1±0.8%
91.0±2.3%
2.1±0.3%
1.7±0.3%
96.2±0.4%
Partner concern
(Allogrooming / Pushing)
Stranger concern
Non-social activity /
Sniffing social targets

1368

1369 **Figure 10. Social relationship in trauma induction determines stress development. (A)**
1370 Social relationship increased emotional impact, evidenced by tail rattling behavior during
1371 trauma induction. **(B–F)** No significant chronic difference was found in Stranger-observing
1372 mice. **(G)** The partner-revisiting test. A stranger mouse (light gray S) and the previously pair-
1373 housed partner (light gray P), both immobilized, were presented as social targets. Pink
1374 rectangle, heating pad. **(H)** Partner-observing mice showed significantly longer allogrooming
1375 or pushing their partners (yellow, % of time spent in partner concern behavior) than either No-
1376 scenario-isolated or Stranger-observing mice. Standard errors were calculated from
1377 bootstrapped data.

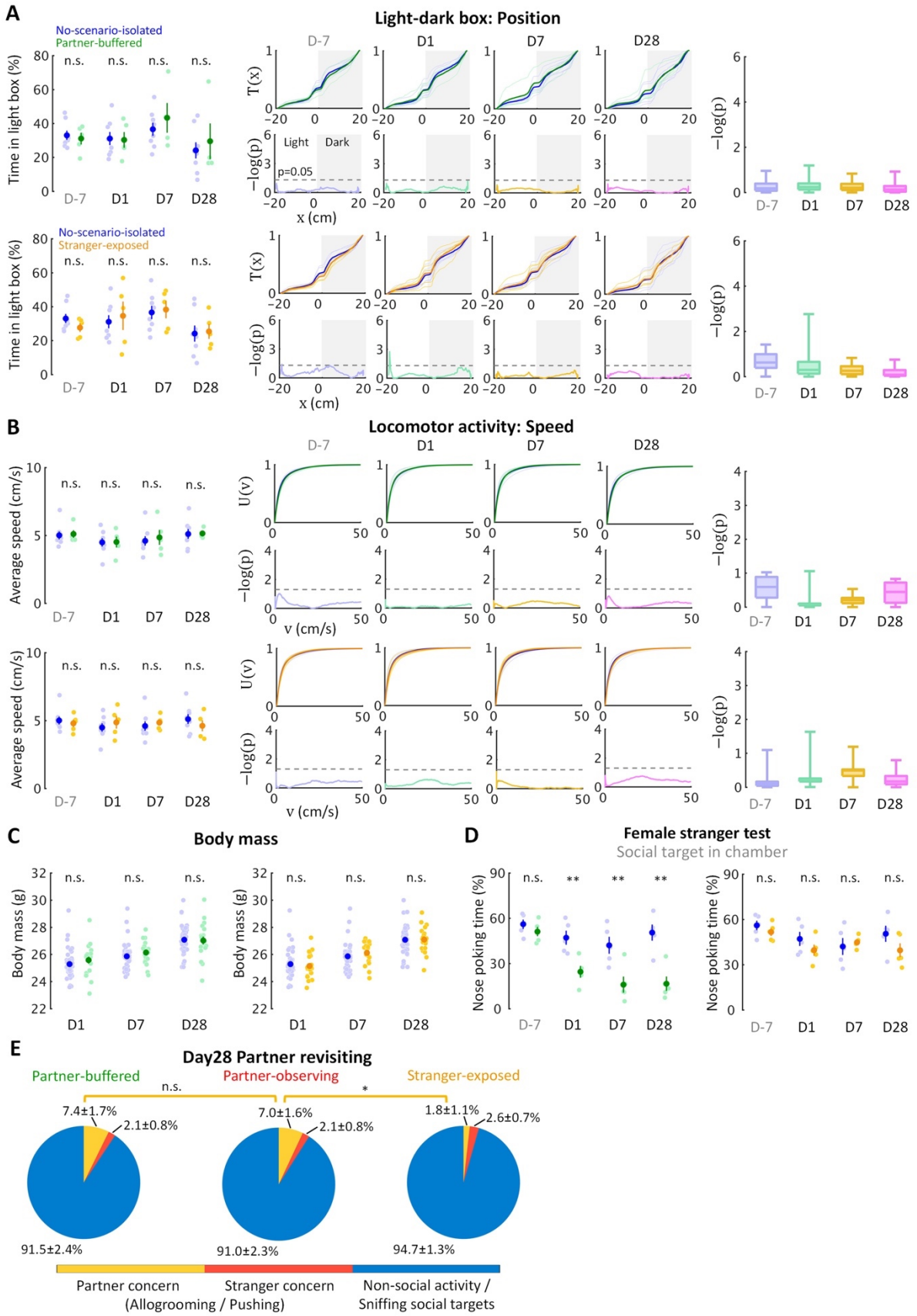
A
Light-dark box: Position
No-scenario-isolated
Partner-buffered
Stranger-exposed
Time in light box (%)
n.s.
D-7
D1
D7
D28
T(x)
−log(p)
Light
Dark
p=0.05
x (cm)
B
Locomotor activity: Speed
Average speed (cm/s)
U(v)
v (cm/s)
C
Body mass
Body mass (g)
D
Female stranger test
Social target in chamber
Nose poking time (%)
**
E
Day28 Partner revisiting
Partner-buffered
Partner-observing
Stranger-exposed
n.s.
*
7.4±1.7%
2.1±0.8%
91.5±2.4%
7.0±1.6%
2.1±0.8%
91.0±2.3%
1.8±1.1%
2.6±0.7%
94.7±1.3%
Partner concern
(Allogrooming / Pushing)
Stranger concern
Non-social activity /
Sniffing social targets

1378

1379 **Figure 11. Control experiments identify necessity of relationship-dependent vicarious**
1380 **defeat and sufficiency of social isolation for anxiety incubation. (A)** Positions in the light-
1381 dark box test indicate that Partner-buffered and Stranger-exposed mice did not develop the
1382 chronic stress reactions. **(B)** Locomotor speeds indicate that Partner-buffered and Stranger-
1383 exposed mice did not develop the acute stress reactions. **(C)** Body masses indicate that Partner-
1384 buffered and Stranger-exposed mice did not develop the physiological differences. **(D)** Nose
1385 poking times in the female stranger test indicate that Partner-buffered mice did, but Stranger-
1386 exposed mice did not develop the social differences. **(E)** Partner-buffered mice and Partner-
1387 observing mice spent longer time on the behaviors reflecting partner concern.

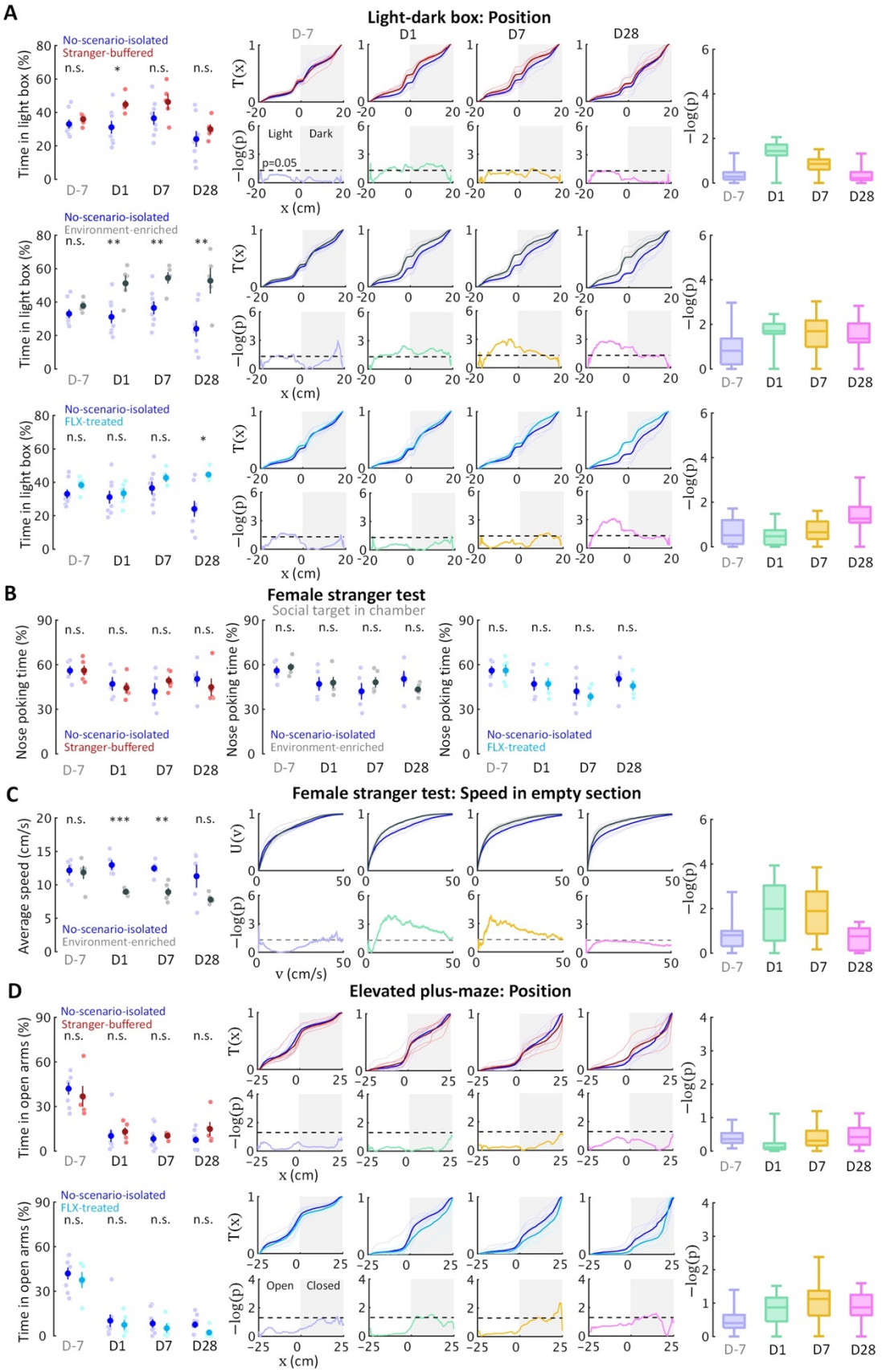
A
Light-dark box: Position
No-scenario-isolated
Stranger-buffered
Environment-enriched
FLX-treated
Time in light box (%)
T(x)
−log(p)
Light
Dark
p=0.05
x (cm)
D-7
D1
D7
D28
B
Female stranger test
Social target in chamber
Nose poking time (%)
C
Female stranger test: Speed in empty section
Average speed (cm/s)
U(v)
v (cm/s)
D
Elevated plus-maze: Position
Time in open arms (%)
Open
Closed
n.s.

1388

1389 **Figure 12. Control experiments uncover that social buffering with non-defeated**
1390 **strangers rescued the full phenotypic dimensions of stress development. (A)** Positions in
1391 the light-dark box test indicate that Environment-enriched and FLX-treated mice did, but
1392 Stranger-buffered mice did not develop the behavioral differences in the late phase. **(B)** Nose
1393 poking times in the female stranger test indicate that Stranger-buffered, Environment-enriched,
1394 and FLX-treated mice did not develop the social differences. **(C)** Environment-enriched mice
1395 showed of reduction in locomotion speed during the non-social phase. **(D)** Positions in the
1396 elevated plus-maze test indicate that Stranger-buffered mice were better rescued than FLX-
1397 treated mice.

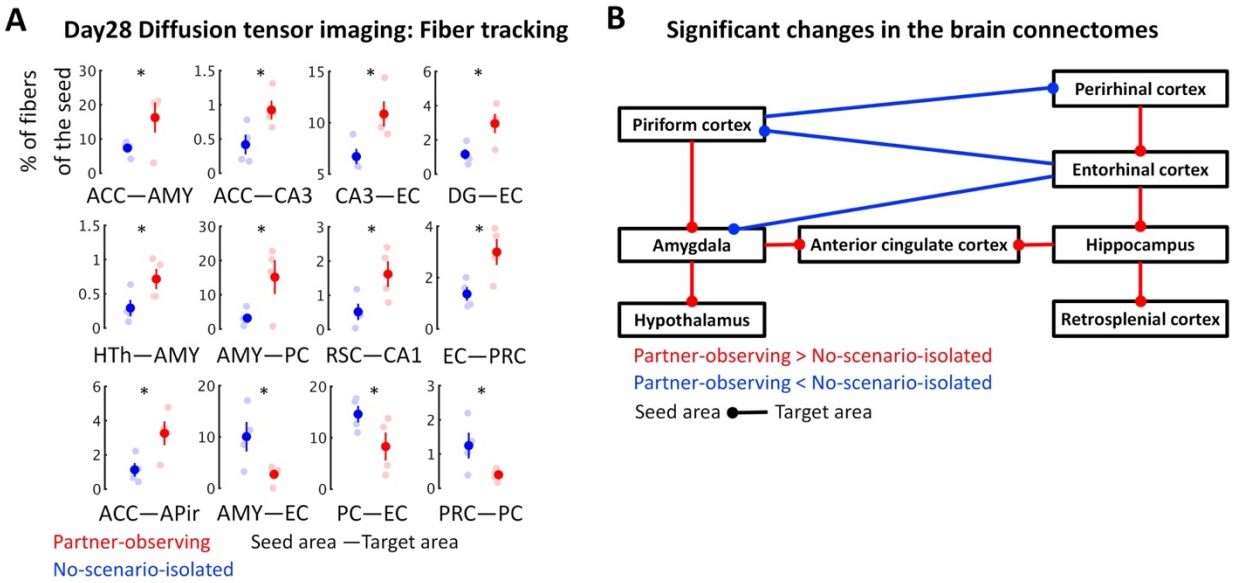

Figure 13. DTI-based long-range connections suggest neural substrate of unitary view for stress development. (A) DTI-based network-wise fiber tracking reveals specific chronic changes of structural connectivity in the brain. AMY, the amygdala; HTh, the hypothalamus; DG, the hippocampal dentate gyrus; PC, the piriform cortex; PRC, the perirhinal cortex; APir, the amygdalopiriform transition area. Note that the brain regions were in the right brain hemisphere. **(B)** Trauma-induced structural changes of the underlying brain connectome uncovered an enhancement of a unitary network centered at the anterior cingulate cortex.

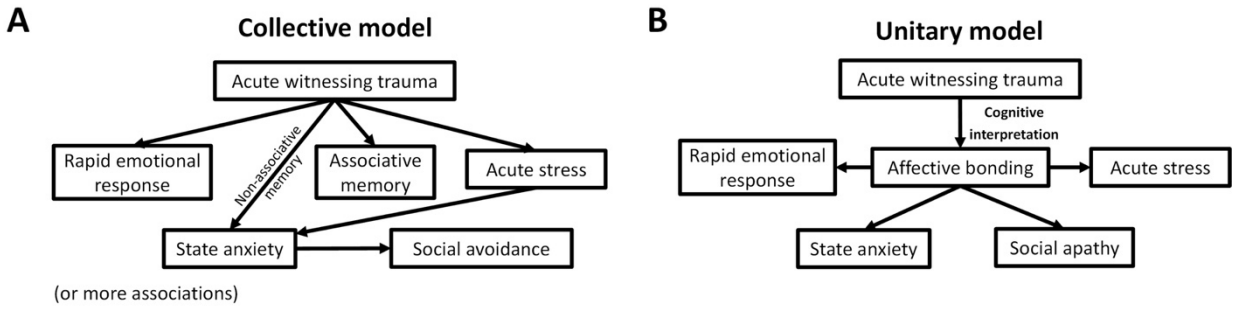

Figure 14. Foregoing data demonstrate a unitary psychopathological model with its corresponding neural substrate for the stress development paradigm in this study. Our data show little support for a collective view speculated in previous hypotheses **(A)**, but support a unitary view **(B)** where diverse PTSD-like reactions independently developed via a common cognitive source ("Affective bonding"). This unitary view suggests a psychological substrate in system-level that integrates multiple mechanisms underlying highly diverse behavioral consequences, as a specific clinical target in the full mechanistic picture.

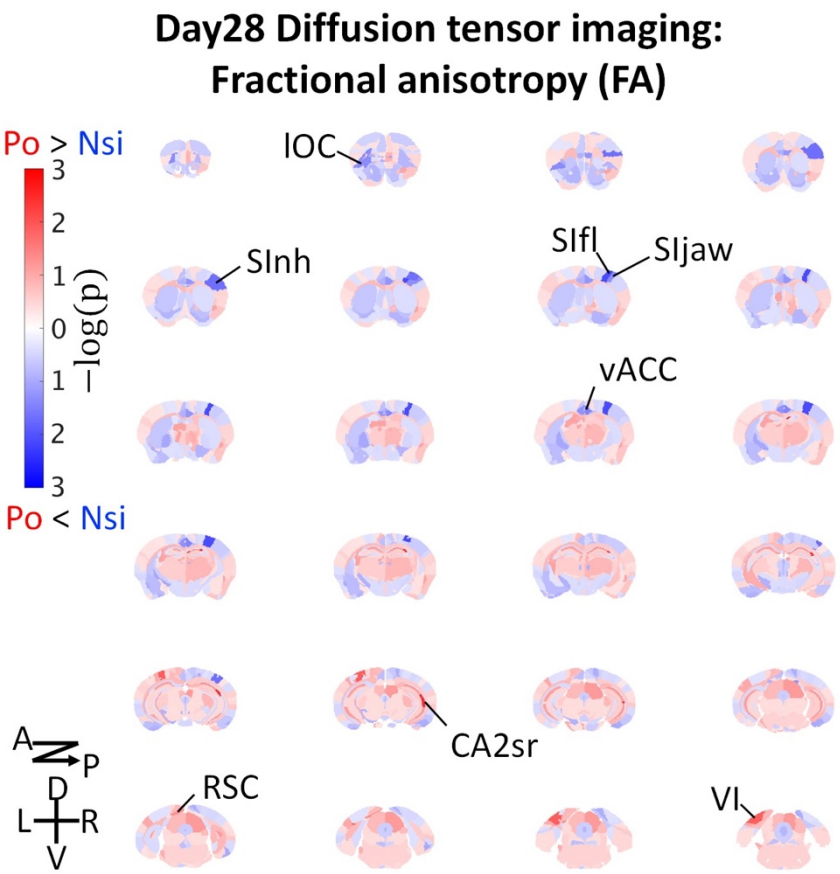

Supplemental Figure 1. Brain-wide microstructural changes measured by DTI fractional anisotropy. Po, Partner-observing mice; Nsi, No-scenario-isolated mice; -log(p), statistical significance through a two-population Student's t-test; A, anterior; P, posterior; D, dorsal; V, ventral; L, left; R, right; lOC, lateral orbital cortex; SInh, non-homunculus region of the primary sensory cortex; SIfl, forelimb region of the primary sensory cortex; SIjaw, jaw region of the primary sensory cortex; vACC, ventral region of the anterior cingulate cortex; CA2sr, stratum radiatum of the hippocampal cornu ammonis (CA) 2 area; RSC, the retrosplenial cortex; VI, the primary visual cortex.

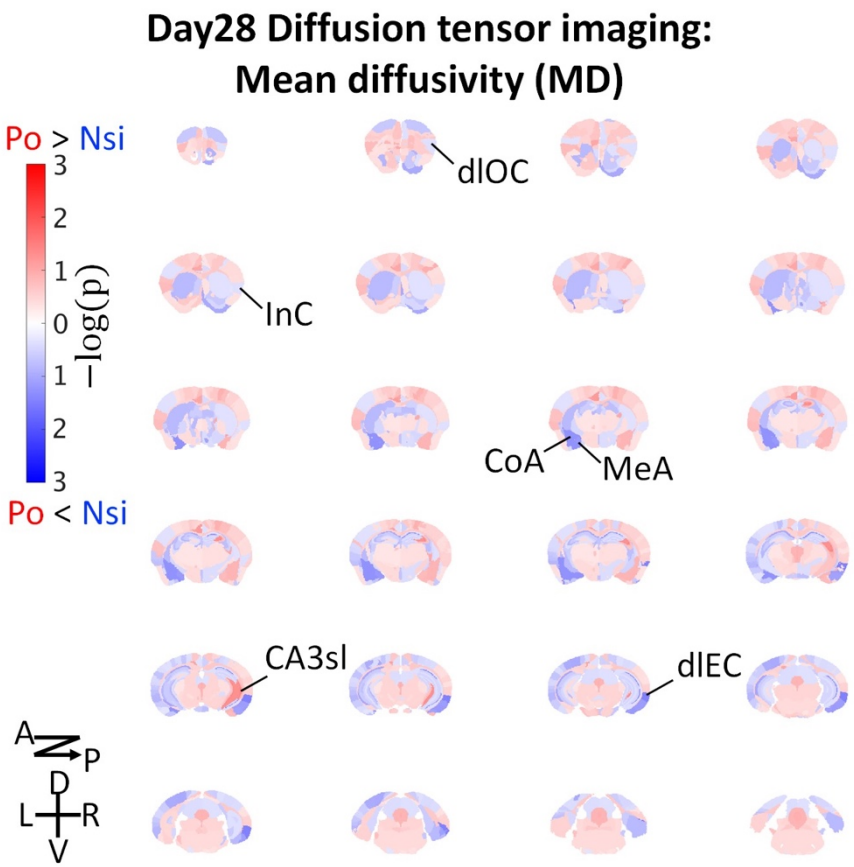

1423

1424 **Supplemental Figure 2. Brain-wide microstructural changes measured by DTI mean**
1425 **diffusivity.** dlOC, dorsolateral orbital cortex; InC, the insular cortex; CoA, the cortical
1426 amygdalar nucleus; MeA, medial amygdalar nucleus; CA3sl, stratum lucidum of the
1427 hippocampal CA3 area; dlEC, dorsolateral entorhinal cortex.

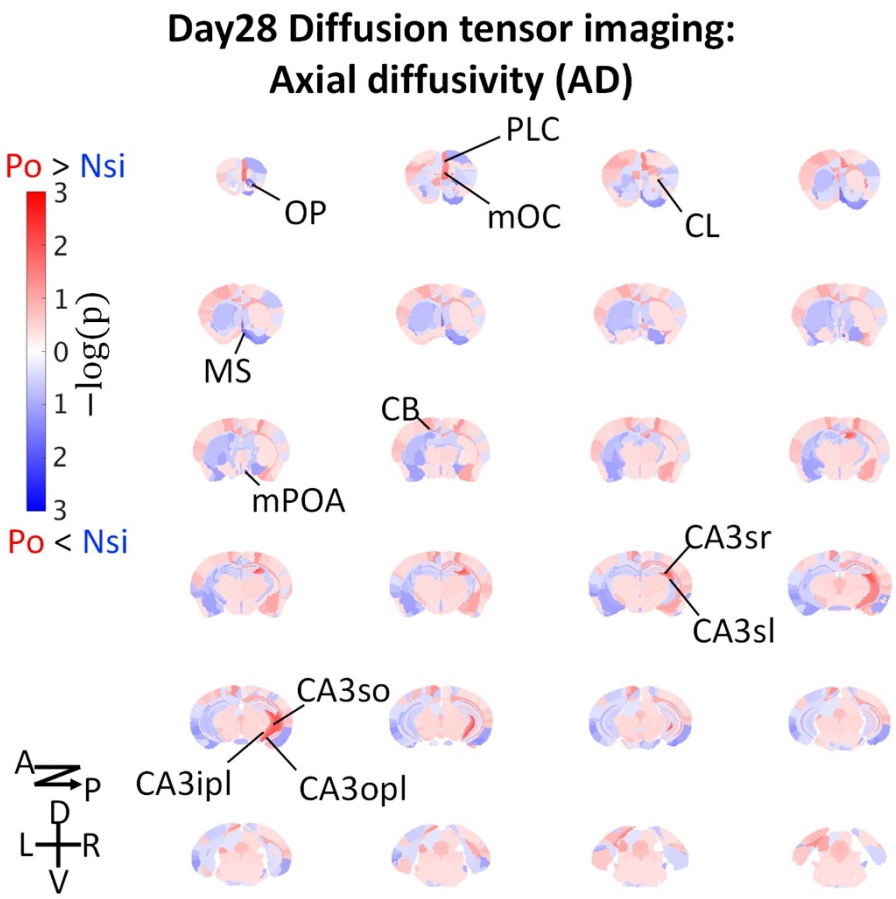

1428

1429 **Supplemental Figure 3. Brain-wide microstructural changes measured by DTI axial**
1430 **diffusivity.** OP, olfactory peduncle; PLC, prelimbic cortex; mOC, medial orbital cortex; CL,
1431 claustrum; MS, medial septal complex; mPOA, medial preoptic area; CB, cingulum bundle;
1432 CA3sr, stratum radiatum of the hippocampal CA3 area; CA3sl, stratum lucidum of the
1433 hippocampal CA3 area;CA3so, stratum oriens of the hippocampal CA3 area; CA3ipl, inner
1434 pyramidal layer of the hippocampal CA3 area; CA3opl, outer pyramidal layer of the
1435 hippocampal CA3 area.

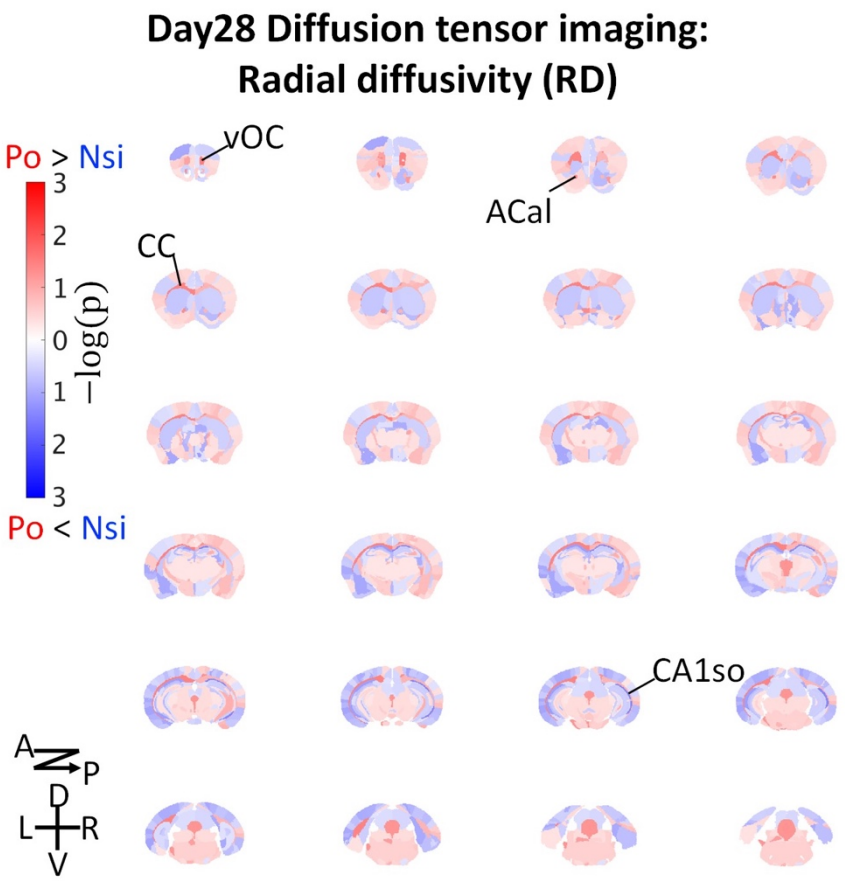

1436

1437 **Supplemental Figure 4. Brain-wide microstructural changes measured by DTI radial**

1438 **diffusivity.** vOC, ventral orbital cortex; ACal, anterior limb of the anterior commissure; CC,

1439 corpus callosum; CA1so, stratum oriens of the hippocampal CA1 area.

1440 **Supplemental Video 1.** Social apathy is an observed behavioral characteristic of Partner-
1441 observing mice. Examples of 30-s recordings during the social session in the female stranger
1442 test on Day1. First scene, No-scenario-isolated mouse; Second scene, Partner-observing mouse.

1443 **Supplement Video 2.** Illustration of behavioral characteristics that were specific to observer
1444 mice during trauma induction when their partners were attacked. First scene, tail rattling during
1445 aggressive encounter; Second scene, tail rattling during aggressive encounter (4x slower);
1446 Third scene, hiding under bedding material with the partner during resting. These behaviors
1447 were not observed if a stranger mouse got attacked.

1448 **Supplemental Video 3.** Illustration of rebound reaction of a Partner-observing mouse to its
1449 previously pair-housed partner during the partner-revisiting test.